

6

AFML-TR-65-2
PART II, VOLUME XVI

AD 664344

TERNARY PHASE EQUILIBRIA IN TRANSITION METAL-BORON-CARBON-SILICON SYSTEMS

**PART II. TERNARY SYSTEMS
Volume XVI. V-Nb-C System**

Y. A. CHANG

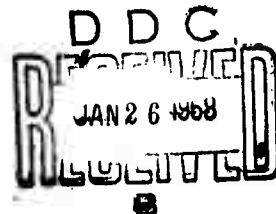
AEROJET-GENERAL CORPORATION

TECHNICAL REPORT No. AFML-TR-65-2, PART II, VOLUME XVI

DECEMBER 1967

Distribution of this document is unlimited. It
may be released to the Clearinghouse, Depart-
ment of Commerce, for sale to the general public.

**AIR FORCE MATERIALS LABORATORY
RESEARCH AND TECHNOLOGY DIVISION
AIR FORCE SYSTEMS COMMAND
WRIGHT-PATTERSON AIR FORCE BASE, OHIO**



Reproduced by the
CLEARINGHOUSE
for Federal Scientific & Technical
Information Springfield Va 22151

65

NOTICES

When Government drawings, specifications, or other data are used for any purpose other than in connection with a definitely related Government procurement operations, the United States Government thereby incurs no responsibility nor any obligation whatsoever; and the fact that the Government may have formulated, furnished, or in any way supplied the said drawings, specifications, or other data, is not to be regarded by implication or otherwise as in any manner licensing the holder or any other person or corporation, or conveying any rights or permission to manufacture, use, or sell any patented invention that may in any way be related thereto.

RECEIVED BY
DATE
TIME
BY
OFFICE
SECTION
NO.
REMARKS
A. J. L. 100-100000

Copies of this report should not be returned unless return is required by security considerations, contractual obligations, or notice on a specific document.

BLANK PAGE

**TERNARY PHASE EQUILIBRIA IN TRANSITION
METAL-BORON-CARBON-SILICON SYSTEMS**

**PART II. TERNARY SYSTEMS
Volume XVI. V-Nb-C System**

Y. A. CHANG

Distribution of this document is unlimited. It may be released to the Clearinghouse, Department of Commerce, for sale to the general public.

FOREWORD

The work described and illustrated in this report was performed at the Materials Research Laboratory, Aerojet-General Corporation, Sacramento, California, under USAF Contract No. AF 33(615)-1249. The contract was initiated under Project No. 7350, Task No. 735001. The work was administered under the direction of the Air Force Materials Laboratory, with Lt. P. J. Marchiando acting as Project Engineer, and Dr. E. Rudy, Aerojet-General Corporation, as Principal Investigator. Professor Dr. Hans Nowotny, University of Vienna, Austria, served as consultant to the project.

The project, which includes the experimental and theoretical investigation of selected refractory ternary systems in the system classes Me_1-Me_2-C , $Me-B-C$, Me_1-Me_2-B , $Me-Si-B$ and $Me-Si-C$, was initiated on 1 January 1964.

The experimental program was laid out by Dr. E. Rudy, and the author wishes to thank him for his advice during the course of this investigation. He further wishes to thank J. R. Hoffman for many helpful discussions with respect to metallographic interpretations, E. Spencer for sample preparation, and R. Cobb for the X-ray exposures and metallographic prints. Finally, the typing of the report by Mrs. J. Weidner and the preparation of the drawings by Mr. R. Cristoni are gratefully acknowledged.

Other reports issued under USAF Contract AF 33(615)-1249 have included:

Part I. Related Binaries

- Volume I. Mo-C System
- Volume II. Ti-C and Zr-C Systems
- Volume III. Systems Mo-B and W-B
- Volume IV. Hf-C System
- Volume V. Ta-C System. Partial Investigations
in the Systems V-C and Nb-C
- Volume VI. W-C System. Supplemental Information
on the Mo-C System
- Volume VII. Ti-B System
- Volume IX. Hf-B System
- Volume X. V-B, Nb-B, and Ta-B Systems
- Volume XI. Final Report on the Mo-C System
- Volume XII. Revision of the V-C and Nb-C Systems

Part II. Ternary Systems

- Volume I. Ta-Hf-C System
- Volume II. Ti-Ta-C System
- Volume III. Zr-Ta-C System
- Volume IV. Ti-Zr-C, Ti-Hf-C, and Zr-Hf-C Systems
- Volume V. Ti-Hf-B System
- Volume VI. Zr-Hf-B System

FOREWORD (Cont'd)

- Volume VII. Systems Ti-Si-C, Nb-Si-C, and W-Si-C
- Volume VIII. Ta-W-C System
- Volume IX. Zr-W-B System. Pseudo-binary System
TaB₂-HfB₂
- Volume X. Systems Zr-Si-C, Hf-Si-C, Zr-Si-B, and
Hf-Si-B
- Volume XI. Systems Hf-Mo-B and Hf-W-B
- Volume XII. Ti-Zr-B System
- Volume XIII. Phase Diagrams of the Systems Ti-B-C,
Zr-B-C, and Hf-B-C
- Volume XIV. The Hafnium-Iridium-Boron System
- Volume XV. Constitution of Ternary Niobium-Molybdenum-
Carbon Alloys


Part III. Special Experimental Techniques

- Volume I. High Temperature Differential Thermal
Analysis
- Volume II. A Pirani-Furnace for the Precision Determina-
tion of the Melting Temperatures of Refractory
Metallic Substances

Part IV. Thermochemical Calculations

- Volume I. Thermodynamic Properties of Group IV, V,
and VI Binary Transition Metal Carbides.
- Volume II. Thermodynamic Interpretation of Ternary
Phase Diagrams
- Volume III. Computational Approaches to the Calculation
of Ternary Phase Diagrams.

This technical report has been reviewed and is approved.


W. G. RAMKE
Chief, Ceramics and Graphite Branch
Metals and Ceramics Division
Air Force Materials Laboratory

ABSTRACT

Phase equilibria in the ternary system vanadium-niobium-carbon from 800°C through the melting ranges of the cubic monocarbide solid solutions have been established on the basis of X-ray, melting point, and metallographic studies. The phase equilibria above 1400°C are presented in a three-dimensional temperature-composition constitutional diagram; the phase equilibria below 1400°C were not extensively investigated due to kinetics problem. Vanadium monocarbide and niobium monocarbide form a continuous solid solution in the same manner as the low-temperature modification of the ordered hexagonal vanadium subcarbide and niobium subcarbide. However, the addition of vanadium subcarbide to niobium subcarbide stabilizes the high-temperature modification of the disordered hexagonal niobium subcarbide to about 1780°C in the ternary field.

TABLE OF CONTENTS

	PAGE
I. INTRODUCTION AND SUMMARY	1
A. Introduction	1
B. Summary.	1
1. Binary Systems	2
2. Constitution Diagram Vanadium-Niobium-Carbon.	2
II. LITERATURE REVIEW	5
A. Boundary Systems	5
B. Vanadium-Niobium-Carbon.	10
III. EXPERIMENTAL PROGRAM	10
A. Experimental Procedures	10
1. Starting Materials.	10
2. Alloy Preparation and Heat Treatment	11
3. Melting Point	14
4. Differential Thermal Analysis	14
5. Metallography.	14
6. X-Ray Analysis	15
7. Chemical Analysis	15
B. Experimental Results	15
1. Solid State Phase Equilibria	15
2. Phase Equilibria in the Melting Range.	21
3. Assembly of the Phase Diagram	32
IV. DISCUSSION	51
References	54

ILLUSTRATIONS

FIGURE		PAGE
1	Constitution Diagram Vanadium-Niobium-Carbon	3
2	V-Nb-C: Isopleth at 35 Atomic % Carbon	6
3	Constitution Diagram Vanadium-Carbon	7
4	Constitution Diagram Niobium-Carbon	8
5	Compositions of Melting Point Samples	11
6	Compositions of Solid-State Samples Heat-Treated at 1730°C and 1500°C	12
7	Compositions of Solid-State Samples Heat-Treated at 1500°C and 810°C	13
8	Compositions of Alloys Metallographically Examined	13
9	Compositions of Alloys and Qualitative (X-ray) Evaluation of the Alloys Equilibrated at 1730°C	16
10	Compositions of Alloys and Qualitative (X-ray) Evaluation of the Alloys Equilibrated at 1500°C	16
11	Lattice Parameters of the Ternary Monocarbide Solid Solution	17
12	Lattice Parameters of the Ternary Hexagonal Subcarbide Solid Solution	19
13	Lattice Parameters of the Ternary Orthorhombic Subcarbide Solid Solution	20
14	DTA-Thermogram of an V-Nb-C (25-40-35) Alloy	22
15	DTA-Thermogram of an V-Nb-C (15-50-35) Alloy	22
16	V-Nb-C: Schematic Illustration of the Optional Reaction Scheme for the Formation of the $\beta'-(V, Nb)_2C$ Phase	23
17	Photomicrograph of a V-Nb-C (70-5-20) Alloy Quenched from About 1670°C	24
18	Photomicrograph of an Arc-Melted V-Nb-C (70-15-15) Alloy	24
19	Photomicrograph of an Arc-Melted V-Nb-C (60-23-17) Alloy	25
20	Compositions and Melting Temperatures of the Metal-Rich Eutectic Trough	26

ILLUSTRATIONS (Cont'd)

FIGURE		PAGE
21	Photomicrograph of an Arc-Melted V-Nb-C (50-35-15) Alloy	27
22	Photomicrograph of an Arc-Melted V-Nb-C (22-65-13) Alloy	27
23	Compositions and Peritectic Temperatures of the Ternary Sub-carbide Phase	28
24	Photomicrograph of a V-Nb-C (37-30-33) Alloy Quenched from About 2500°C.	29
25	Photomicrograph of a V-Nb-C (15-55-30) Alloy Quenched from About 2500°C.	30
26	Photomicrograph of a V-Nb-C (7-60-33) Alloy Quenched from About 2800°C.	30
27	Pirani Melting Point Data of the Ternary Monocarbide Alloys	31
28	Photomicrograph of a V-Nb-C (5-55-40) Alloy Quenched from About 2600°C.	33
29	Photomicrograph of a V-Nb-C (5-50-45) Alloy Quenched from about 3300°C.	33
30	Compositions and Melting Temperatures of the Carbon-Rich Eutectic Trough	34
31	Photomicrograph of a V-Nb-C (46-4-50) Alloy Quenched from 2650°C	35
32	Photomicrograph of a V-Nb-C (3-40-57) Alloy Quenched from 3200°C.	35
33-46	V-Nb-C: Isothermal Phase Equilibria from 1400°C to 3310°C	36-49
47	V-Nb-C: Liquidus Projections	50

BLANK PAGE

I. INTRODUCTION AND SUMMARY

A. INTRODUCTION

Apart from theoretical interest, phase equilibrium data of binary and ternary alloy systems are essential in preselecting compatible material systems for industrial applications. Although phase diagrams provide only equilibrium data concerning the alloy systems in question, the investigations usually yield valuable information with respect to the kinetics of reaction. Due primarily to their refractoriness, the transition metal carbides have received considerable interest from industrial concerns in recent years. The two binary group V transition metal (vanadium and niobium) carbon systems have been recently thoroughly reinvestigated by Rudy, Windisch, and Brukl⁽¹⁾ of this laboratory; however, high-temperature phase relationships concerning the ternary vanadium-niobium-carbon system are not available in the literature. The present study was undertaken to establish the phase equilibria in this system from 800°C all the way through the melting ranges, since certain vanadium-niobium-carbon alloys have been thought to be potential cutting tool materials.

B. SUMMARY

The ternary alloy system vanadium-niobium-carbon has been investigated by X-ray, metallographic, melting point, and DTA methods. The melting point samples of the ternary alloys were prepared exclusively by hot-pressing in graphite dies, using the monocarbides and the necessary elemental components as the starting materials. Selected, post-melting samples were examined metallographically and arc-melted whenever necessary.

Solid state samples were also prepared by hot-pressing in graphite dies using the elemental components as the starting materials. These samples were heat treated at 810°C, 1500°C, and 1730°C and were examined using X-rays in order to establish the solid-state phase equilibria.

1. Binary Systems

The two, binary metal carbon systems have been recently thoroughly re-investigated by Rudy, Windisch, and Brukl⁽¹⁾, and needs no further discussion here. Earlier works concerning the binary vanadium-niobium system have been summarized by Hansen and Anderko⁽²⁾. More recently, Rudy⁽³⁾ redetermined the melting equilibria and found the system has a minimum congruent melting point, 1862°C at 21 atomic % niobium.

2. Constitution Diagram Vanadium-Niobium-Carbon

The constitution diagram vanadium-niobium-carbon established experimentally, is presented in Figure 1. The main features of this system are described in the following:

a. The Monocarbide Phase

Vanadium monocarbide and niobium monocarbide, both having the B-1 type of structure and large ranges of homogeneity with respect to carbon, form a continuous series of solid solutions at 1500°C. At 45 atomic % carbon, the lattice parameters increase from 4.159 Å at the vanadium side to 4.457 Å at the niobium side, exhibiting a slight positive deviation from Vegard's law. Based on the distribution of the tie lines in the monocarbide-subcarbide two-phase field, a thermodynamic evaluation indicates this phase would form a miscibility gap at about 800°C.

b. The Subcarbide Phase

The orthorhombic forms of V_2C ($a = 11.49 \text{ Å}$, $b = 10.06 \text{ Å}$, and $c = 4.55 \text{ Å}$) stable below about 800°C⁽⁴⁾, and Nb_2C ($a = 12.36 \text{ Å}$, $b = 10.90 \text{ Å}$, and $c = 4.97 \text{ Å}$) stable below about 1200°C⁽⁴⁾, probably form a continuous series of solid solutions based on the lattice parameters of long-time heat-treated samples at about 810°C. The carbon contents of all these alloys were close to 33 atomic %. Both the vanadium-rich and niobium-rich alloys showed the presence of the orthorhombic (ζ -Fe₂N type) structure, while the alloys

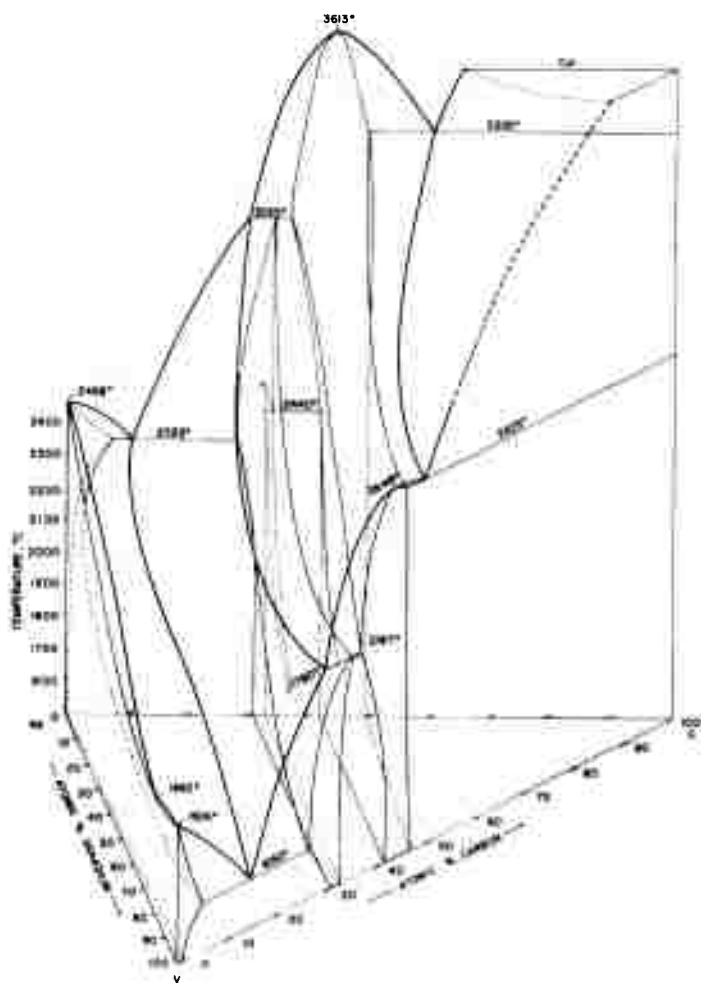


Figure 1. Constitution Diagram Vanadium-Niobium-Carbon

having metal exchanges between 10 to 60 atomic % niobium exhibited only the high-temperature hexagonal structure, presumably never attained equilibrium. The variation of the lattice parameters as a function of metal exchange suggests a continuous series of solid solutions. All the three lattice parameters show positive deviations from linear relationships.

The high-temperature hexagonal forms of V_2C and Nb_2C (ϵ - Fe_2N type) also form a continuous series of solid solutions based on the lattice parameters of the alloys heat treated at 1500 C. The c-parameter increases from 4.57 Å at the vanadium-side to 4.96 Å at the niobium side, while the a-parameter varies from 2.89 Å to 3.15 Å. Both parameters exhibit slight positive deviations from linear relationships. Based on the tie line distributions in the metal-subcarbide two-phase field, a thermodynamic analysis indicates a critical temperature for the formation of a miscibility gap at about 900°C.

In the Nb_2C phase, at about 2440°C, the hexagonal ϵ - Fe_2N type structure of β - Nb_2C undergoes a second phase transformation to γ - Nb_2C as detected by DTA method⁽¹⁾. This transformation is presumably one of sublattice order-disorder transformation as discussed by Rudy and Brukl⁽⁴⁾. The DTA-results of several alloys containing 35 atomic % carbon showed that the addition of vanadium stabilizes the high temperature disorder form to about 1780°C at a metal-exchange of about 62 atomic % niobium.

c. Metal-Rich and Carbon-Rich Equilibria

There is no four-phase reaction in the vanadium-niobium-carbon system. The metal-rich eutectic trough extends from the vanadium-side with 15 atomic % carbon to the niobium side with 7 atomic % carbon. The eutectic temperature increases gradually at first from 1650°C in the vanadium-carbon binary. At a metal-exchange beyond about 30 atomic % niobium, the temperature increases more steeply to 2350°C in the niobium-carbon binary.

Due to the formation of a continuous series of solid solutions of the subcarbide phase at high temperature, the peritectic trough extends from the binary vanadium-carbon to the niobium-carbon side. The temperature increases smoothly from 2187°C to 3035°C.

The carbon-rich eutectic trough between the monocarbide solid solution and graphite extends from the vanadium side with 49.5 atomic % carbon to the niobium side with 60 atomic % carbon. Starting from the vanadium side, the temperature increases gradually from 2625°C up to a metal exchange of about 50 atomic % niobium and then increases sharply to 3300°C.

An isopleth at a 35 atomic % carbon is shown in Figure 2.

II. LITERATURE REVIEW

A. BOUNDARY SYSTEMS

The literature data concerning the phase relationships of both vanadium-carbon and niobium-carbon binary systems up to 1963 were summarized by Kieffer and Benesovsky⁽⁵⁾. More recently, in connection with their reinvestigation of these two binary systems, Rudy, Windisch, and Brukl⁽¹⁾ summarized the newer experimental data. The revised phase diagrams for vanadium-carbon and niobium-carbon according to Rudy et al.⁽¹⁾ are shown in Figures 3 and 4.

In the binary system vanadium-carbon, the metal-rich eutectic containing 15 atomic % C melts at 1650°C. The solubility of carbon in the primary vanadium solid solution at this temperature is 5.5 atomic % C. Vanadium subcarbide (V_2C), having a range of homogeneity from 27 to about 33 atomic % C at 1650°C, melts peritectically at 2187°C to the monocarbide phase and a melt containing about 29 atomic % C. The monocarbide (VC), having a large range of homogeneity from 37 to about 46.5 atomic % C at 2200°C, melts with a

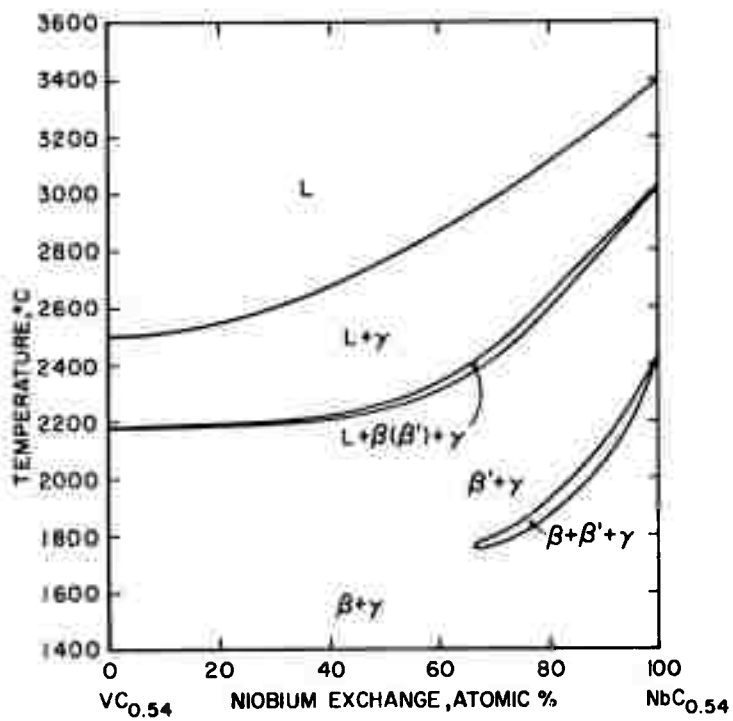


Figure 2. V-Nb-C: Isopleth at 35 Atomic % Carbon

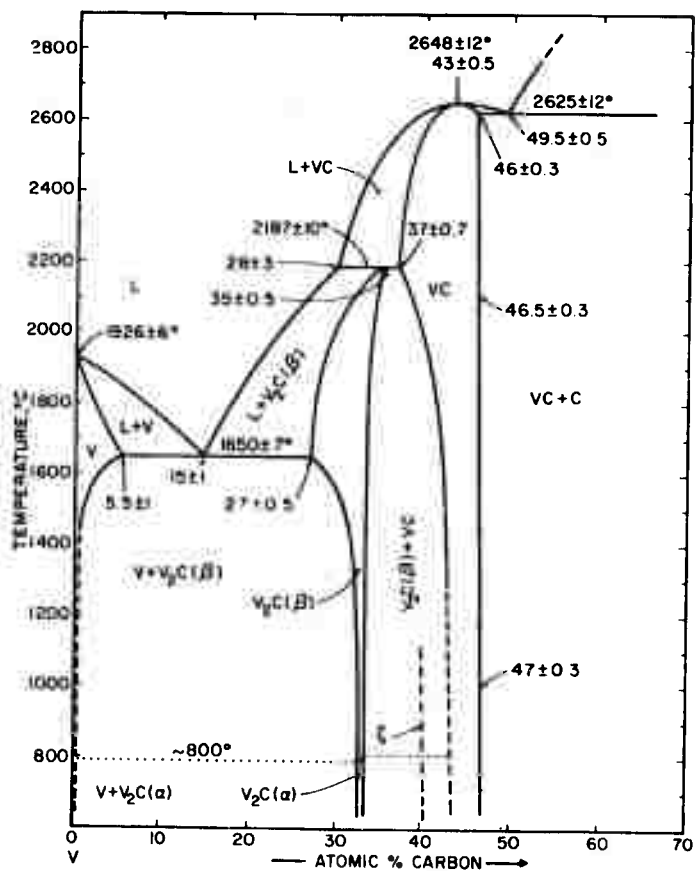


Figure 3. Constitution Diagram Vanadium-Carbon .
(E. Rudy, St. Windisch, and C. E. Brukl)

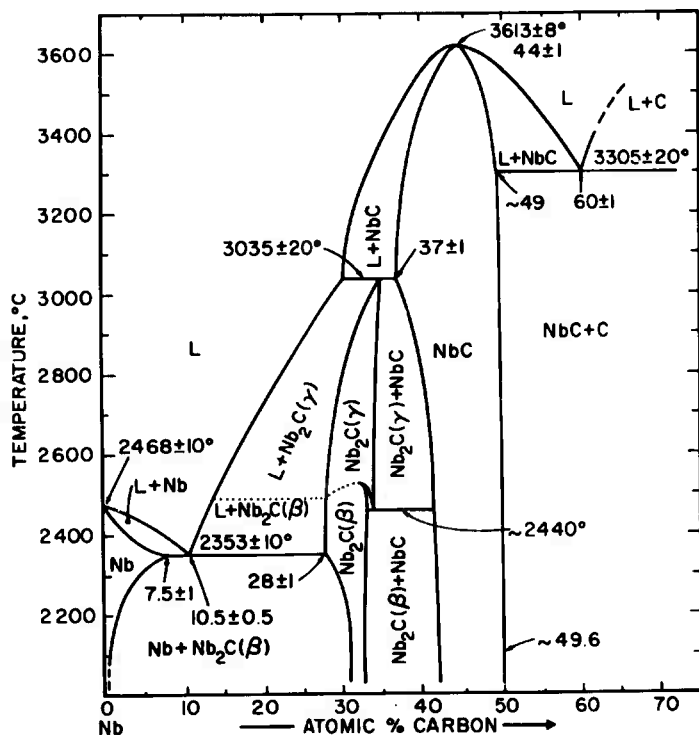


Figure 4. Constitution Diagram Niobium-Carbon .
(E. Rudy, St. Windisch, and C. E. Brühl).

maximum at 2648°C and 43 atomic % C. The monocarbide-graphite eutectic, with 49.5 atomic % C, melts at 2625°C. Above about 800°C, vanadium sub-carbon has a hexagonal (undistorted) structure (β - V_2C). The lattice parameters vary from $a = 2.884 \text{ \AA}$ and $c = 4.565 \text{ \AA}$ at the metal-rich boundary to $a = 2.901 \text{ \AA}$ and $c = 4.575 \text{ \AA}$ at the carbon-rich boundary. At about 800°C, the high temperature hexagonal modification (β - V_2C) undergoes a homogeneous phase transformation to an ordered, orthorhombic modification (ζ - Fe_2N type) α - V_2C . The lattice parameters of this modification are $a = 11.49 \text{ \AA}$, $b = 10.96 \text{ \AA}$, and $c = 4.55 \text{ \AA}$. The transition proceeds sluggishly and even more so when monocarbide is present. The ζ -phase described earlier by Storms

and McNeal⁽⁶⁾ has not been thoroughly studied by Rudy et al. to be certain whether it is a stable or metastable phase analogous to the phase in the tantalum-carbon system⁽⁷⁾. The lattice parameters of the monocarbide B-1 phase vary linearly with the carbon content.

With the exception of the subcarbide phase (Nb_2C), the general phase relationships in the binary system niobium-carbon are similar to those in the vanadium-carbon system. The metal-rich eutectic at a carbon concentration of 10.5 atomic % melts at 2353°C. The maximum solubility of carbon in the primary metal solid solution at the eutectic temperature is 7.5 atomic % C. There are three polymorphic modifications of the niobium subcarbide phase (Nb_2C). At temperatures below about 1230°C, $\alpha\text{-Nb}_2\text{C}$ has the orthorhombic $\zeta\text{-Fe}_2\text{N}$ type structure ($a = 12.36 \text{ \AA}$, $b = 10.90 \text{ \AA}$, and $c = 4.97 \text{ \AA}$). Above this temperature, $\beta\text{-Nb}_2\text{C}$ has the hexagonal structure (probably $\epsilon\text{-Fe}_2\text{N}$ type) and the lattice parameters vary from $a = 3.117 \text{ \AA}$, $c = 4.956 \text{ \AA}$ to $a = 3.127 \text{ \AA}$, $c = 4.974 \text{ \AA}$ at the carbon-rich phase boundary. With increasing temperature to about 2440°C (referring to Figure 3), the hexagonal $\beta\text{-Nb}_2\text{C}$, an ordered phase, reacts with the monocarbide phase at a eutectoid isotherm to form the high-temperature disordered form of $\gamma\text{-Nb}_2\text{C}$. The ordered hexagonal substoichiometric Nb_2C phase undergoes a second-order phase transformation to the high-temperature disordered structure with a destruction of long-range order in the carbon sublattice. In a similar manner as V_2C , Nb_2C melts peritectically at 3035°C to the monocarbide phase and a melt containing about 28 atomic % C. The ζ -phase which was claimed to be a third intermediate phase between the subcarbide and monocarbide phases⁽⁸⁾ has been shown by Rudy et al.⁽¹⁾ to be a metastable phase within the temperature range 1600° to 2500°C. The monocarbide B-1 phase (NbC), having a large range of homogeneity from 37 to 49 atomic % C at 3035°C, melts with a maximum at 3613°C and 44 atomic % C. NbC forms an eutectic with graphite at 3305°C and 60 atomic % C. The lattice parameter of NbC phase increases from $a = 4.431 \text{ \AA}$ to 4.470 \AA at the carbon-rich boundary, exhibiting a positive deviation from a linear relationship.

Earlier works concerning the binary vanadium-niobium system have been summarized by Hansen and Anderko⁽²⁾. More recently

Rudy⁽³⁾ redetermined the melting points of this binary system using high-purity metal powders. He found this system has a minimum congruent melting point at 1862°C and 21 atomic % Nb.

B. VANADIUM-NIOBIUM-CARBON

With the exception of the calculated phase diagram of the system vanadium-niobium-carbon at 1700°C by Rudy⁽⁹⁾, no experimental data exist in the literature.

III. EXPERIMENTAL PROGRAM

A. EXPERIMENTAL PROCEDURES

1. Starting Materials

The melting point samples were prepared from vanadium monocarbide, niobium monocarbide, and the elemental powders. Both monocarbides were prepared by directly reacting the cold-pressed metal powders in a carbon pot furnace. The vanadium powder used for preparing the starting monocarbide material was purchased from Oregon Metallurgical Corporation. The impurities in ppm were: C-350, H₂-32, O₂-1780, N₂-320, Fe-950, and Si-460. Niobium metal powder was purchased from Wah Chang Corporation and had the following impurities in ppm: Al-<20, C-30, Fe-42, H₂-210, N₂-115, O-940, Si-<50, Ta-<50, and Ti-<40. The carbon powder, purchased from National Carbon Company, had the following impurities in ppm: S-110, Si-46, Ca-44, Fe-40, Al-8, Ti-4, and Mg-2. Since the metal-carbon mixtures were reacted at rather high temperature under vacuum, the impurity oxygen reacted with graphite to form volatile CO. Chemical analyses of the two monocarbide starting materials showed that VC had 17.77 wt% C (47.8 atomic % C) while NbC had 10.68 wt% C (48.05 atomic % C). The lattice parameters of VC and NbC determined from powder patterns using Cu-K α radiation were $a = 4.162 \text{ \AA}$ and 4.468 \AA , respectively.

For solid state investigations, samples were prepared from the elemental powders.

2. Alloy Preparation and Heat Treatment

The cylindrical melting point samples of approximately 13 mm in diameter and 30 mm in length with a rectangular or cylindrical reduced section in the center were prepared by hot-pressing well-mixed powder mixtures in graphite dies. Before determining the melting points of these alloys, the hot-pressed samples were ground on sandpaper to remove any minute surface contaminations. A small hole of 1 mm diameter, drilled into the center portion of the samples, served as the black-body cavity for the temperature measurements. The compositions of all the melting point samples are shown in Figure 5.

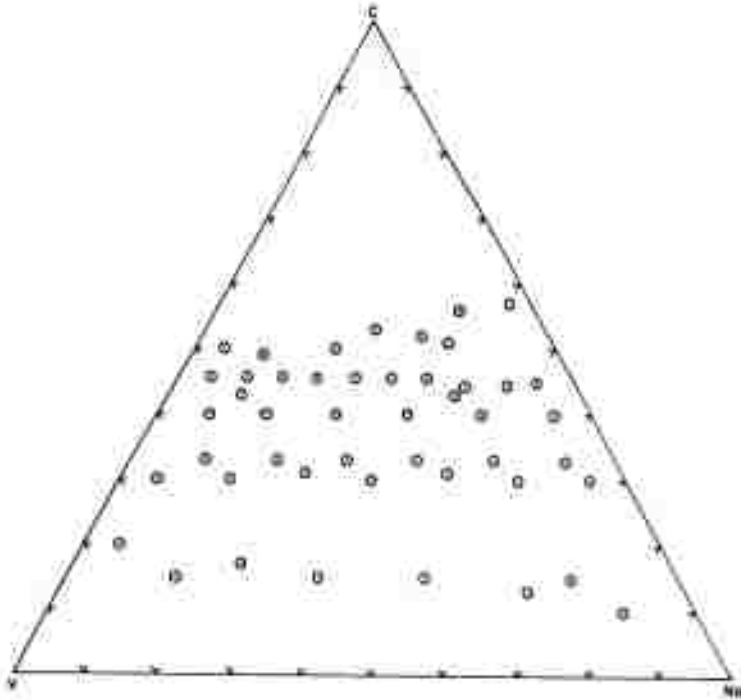


Figure 5. Compositions of Melting Point Samples.

For solid-state investigations, samples having the approximate dimensions of 8 mm in diameter and 6 mm in height were likewise hot-pressed in graphite dies using well-mixed elemental powders. After hot-pressing, each sample was surface-ground to remove any contamination before long-time heat treatment was carried out to achieve equilibrium. The alloys having carbon compositions higher than 30 atomic % C were heat-treated at 1730°C for 60 hours and selected alloys were also heat treated at 1500°C for 90 hours as shown in Figure 6. Both heat treatments were carried out in an atmosphere of high-purity helium. As shown in Figure 7, alloys having a carbon composition less than 35 atomic % C were first heat-treated at 1500°C for 64 hours under an atmosphere of helium. Among these alloys, selected compositions were also heat-treated at 810°C under high vacuum ($\sim 1 \times 10^{-5}$ mm Hg) for a period of 300 hours.

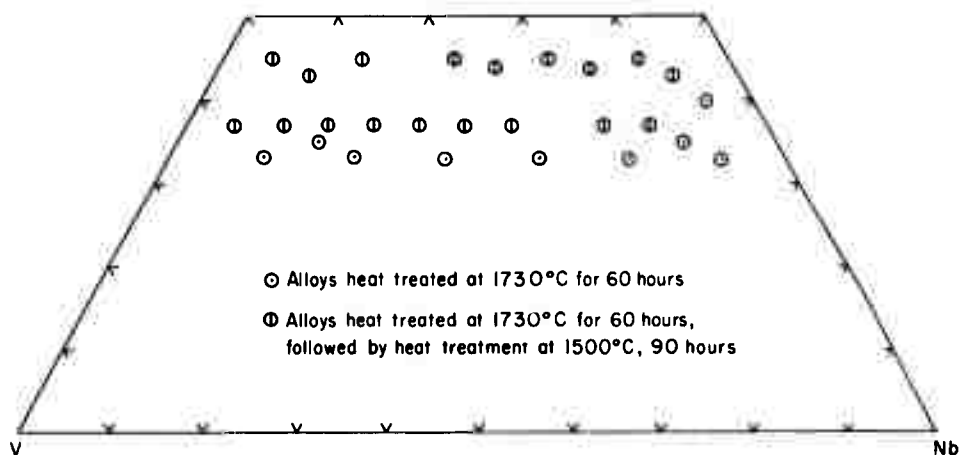


Figure 6. Compositions of Solid-State Samples Heat-Treated at 1730°C and 1500°C.

Whenever the melting point samples were not sufficiently dense for metallographic examination, they were arc melted in a non-consumable tungsten electrode melting furnace. The samples were then examined both by X-ray and metallographic methods. The compositions of all the alloys metallographically examined are shown in Figure 8.

- Alloys heat treated at 1500°C for 64 hours
- ⊙ Alloys heat treated at 1500°C for 64 hours,
followed by heat treatment at 810°C, 300 hours

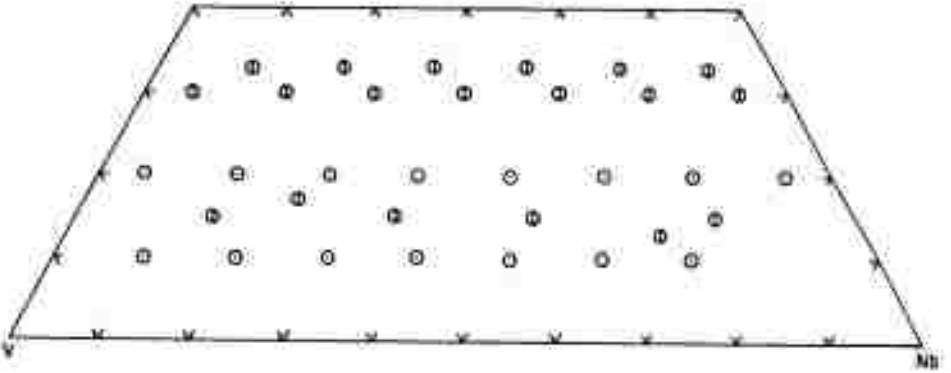


Figure 7. Compositions of Solid-State Samples Heat-Treated at 1500°C and 810°C.

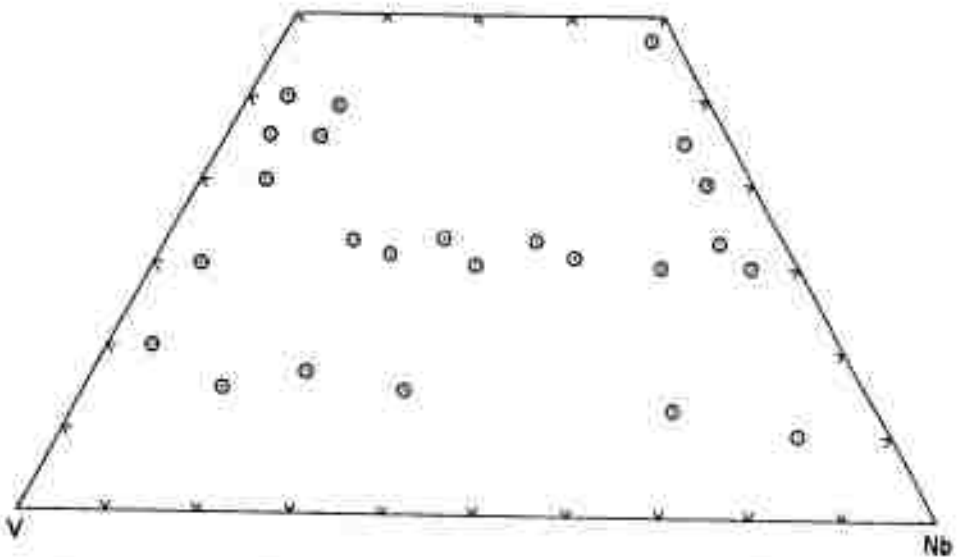


Figure 8. Compositions of Alloys Metallographically Examined.

3. Melting Point

The melting point determinations of selected alloys, as shown in Figure 4, was carried out using the Pirani-technique which has been extensively described previously⁽¹⁰⁾.

The temperature measurements were carried out with a disappearing filament type micropyrometer, which was calibrated against a certified lamp from the National Bureau of Standards. The temperature was corrected for absorption losses in the quartz window of the melting point furnace and deviations due to non-black-body conditions of the observation hole. The detailed treatment with regard to the temperature correction has also been discussed by Rudy and Progulski⁽¹⁰⁾ and needs no further discussion here.

To prevent any appreciable loss of carbon or metal components from the melting samples during the course of the melting point determination, the furnace chamber was pressurized to about 2-1/4 atmospheres with high purity helium after a short vacuum degassing treatment at temperatures below the incipient melting points.

4. Differential Thermal Analysis

The details of DTA-apparatus has been discussed extensively in previous publications⁽¹¹⁾ and will not be repeated here.

5. Metallography

The metallographic samples, which had been either a small portion of the molten zone of the melting point samples, or are melted samples whenever the molten zone of the melting sample was not sufficiently dense, were mounted in an electrically conductive mixture of diallylphtalate-lucite-copper powder. After coarse grinding on silicon carbide paper with grit sizes varying from 120 to 600, the samples were first polished on a nylon cloth using a slurry of 5% chromic acid and 3 μ alumina powder. After all

these treatments, alloys having carbon concentrations more than 49 atomic % (see Figure 8) were ready to be photomicrographed directly due to the large contrast between the graphite precipitates and the monocarbide phase. For alloys between 35 to 49 atomic % C, the specimens were then electroetched with 5% sulfuric acid. Finally, for alloys having carbon concentrations less than 35 atomic %, niobium-rich specimens were electroetched with 0.5% oxalic acid while the vanadium-rich specimens were dipped in 20% Murakami's solution before photomicrographs were taken.

6. X-Ray Analysis

Debye-Scherrer powder diffraction patterns, using Cr-K α radiation, were made of all samples after melting point and solid state investigations, as well as of arc melted samples.

7. Chemical Analysis

The two starting monocarbide materials, vanadium and niobium monocarbides, were analyzed for carbon concentration using the direct combustion method. The carbon content was determined by measuring the thermal conductivity of the combusted CO₂-O₂ gas mixture in a Leco carbon analyzer.

B. EXPERIMENTAL RESULTS

1. Solid State Phase Equilibria

The phase equilibria of the ternary system vanadium-niobium-carbon, as determined primarily from an X-ray analysis of the long-time heated samples at 1730°C and 1500°C, are shown in Figures 9 and 10. Since the subcarbide and monocarbide solid solutions melt at relatively high temperatures, they were heat treated at 1730°C under helium in order to achieve equilibrium. At this temperature, VC and NbC form a continuous series of solid solutions as evidenced by the continuous variation of the lattice

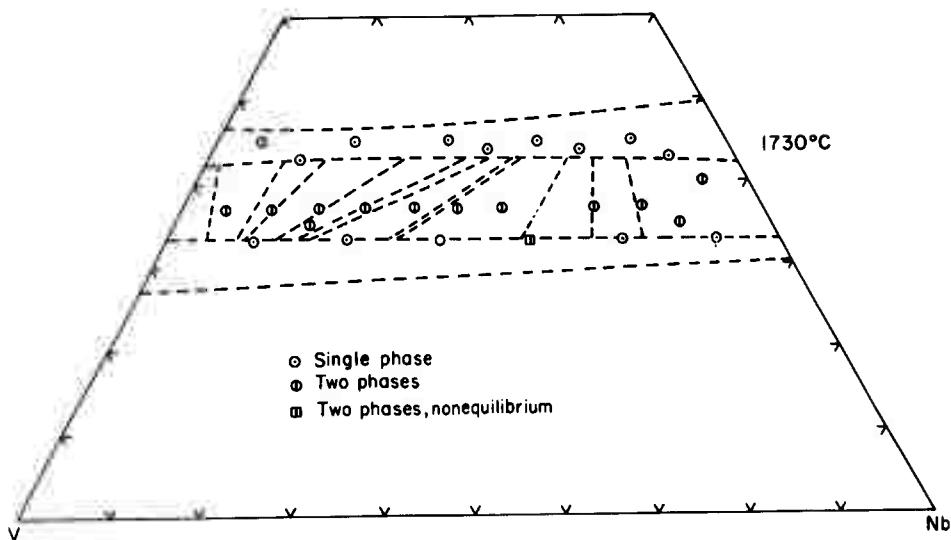


Figure 9. Compositions of Alloys and Qualitative (X-ray) Evaluation of the Alloys Equilibrated at 1730°C.

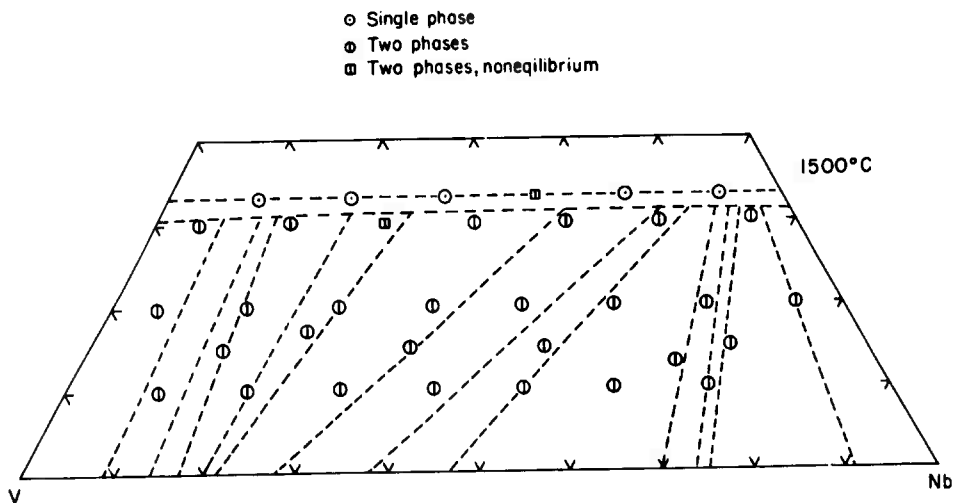


Figure 10. Compositions of Alloys and Qualitative (X-ray) Evaluation of the Alloys Equilibrated at 1500°C.

parameters in terms of metal exchange as shown in Figure 11. The lattice parameters were obtained at room temperature on alloys quenched from 1730°C. As shown in Figure 11, the lattice parameter increases from $a = 4.159 \text{ \AA}$ at the vanadium-side to $a = 4.457 \text{ \AA}$ at the niobium-side, exhibiting a positive deviation from the Vegard's law. Selected alloys in the sub-carbide-monocarbide region (see Figure 6) were then heat treated at 1500°C under helium for 90 hours to see whether a miscibility gap results in the monocarbide solid solution. The lattice parameters of all these alloys quenched from 1500°C were essentially the same as those quenched from 1730°C as mentioned earlier, indicating, at least at 1500°C, VC and NbC still form a continuous series of solid solutions.

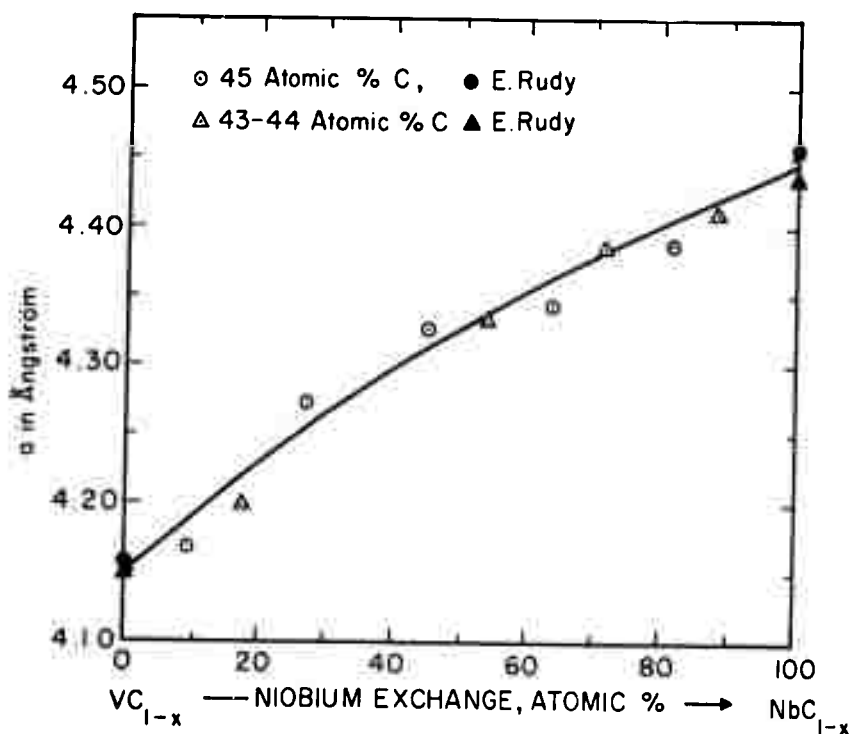


Figure 11. Lattice Parameters of the Ternary Monocarbide Solid Solution .

The continuous variation of lattice parameters of the hexagonal subcarbide alloys quenched from 1500°C are shown in Figure 12 as a function of metal exchange, indicating that V_2C and Nb_2C also form a continuous series of solid solutions. The c-parameter increases from 4.58 Å to 4.96 Å; while the a-parameter increases from 2.89 Å to 3.14 Å. Both exhibit positive deviation from linear relationships. The c/a ratio increases slightly from V_2C to Nb_2C . The lattice parameters of the pure hexagonal V_2C and Nb_2C were taken from the compilation of Storms⁽⁸⁾. Alloys in the subcarbide region, as well as selected ones in the metal-subcarbide two-phase field (Figure 7), were heat treated at 810°C for 300 hours under a vacuum of $\sim 1 \times 10^{-5}$ mm Hg. X-ray examinations of these alloys showed most of the niobium-rich alloys transformed to the low-temperature orthorhombic structure. The lattice parameters of all the alloys transformed to the low-temperature structure are plotted as a function of niobium-exchange in Figure 13. Based on the variations of these lattice parameters, it is believed that V_2C and Nb_2C of the orthorhombic structure also form a continuous series of solid solutions at about 810°C. Since none of the subcarbide alloys within 10 to 60 atomic % Nb showed any evidence of the low-temperature orthorhombic structure, they presumably never attained the equilibrium, and the center portions of the lattice parameter versus composition curves are drawn as dashed lines.

As shown in Figures 9 and 10, the tie-line distributions within the metal-subcarbide and subcarbide-monocarbide two-phase fields at 1500°C and 1730°C, respectively, were determined by comparing the lattice parameters of the component phases present in the two-phase alloys with the variations of the lattice parameters of the three series of solid solutions. The lattice parameters of the body-centered cubic metal solid solutions were determined by Wilhelm, Carlson, and Dickinson⁽¹²⁾, while the lattice parameters of the hexagonal subcarbide and the cubic monocarbide solid solutions are those obtained in the present study.

Since there is no corresponding high-temperature modification of the γ - Nb_2C structure in the V_2C phase, the effect of V_2C addition to the transformation of β - Nb_2C to γ - Nb_2C has been studied by DTA-technique. DTA thermograms of two ternary alloys: V-Nb-C (25-40-35) and V-Nb-C

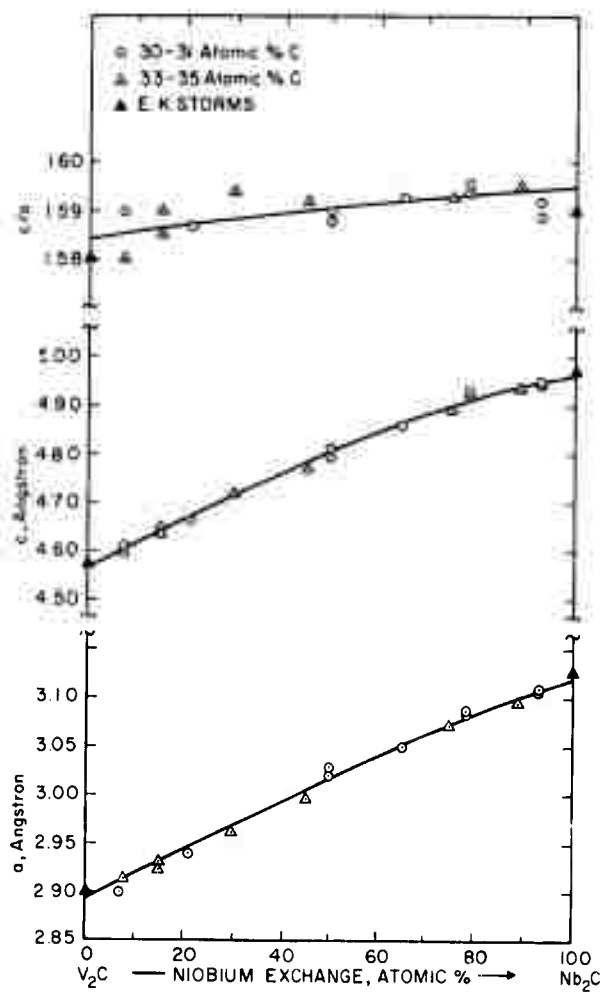


Figure 12. Lattice Parameters of the Ternary Hexagonal Subcarbide Solid Solution .

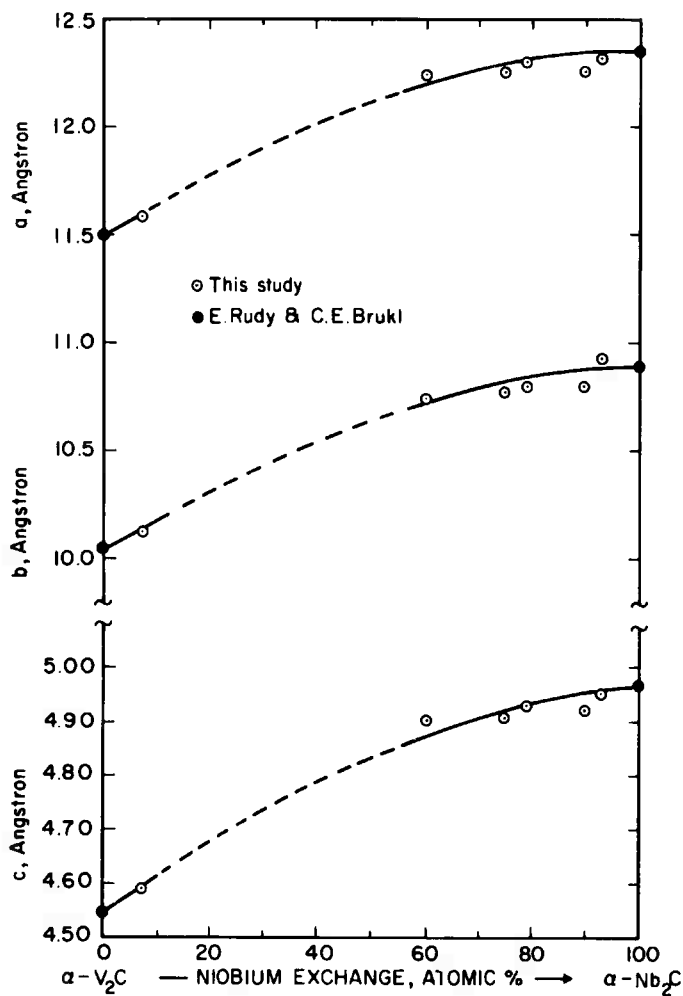


Figure 13. Lattice Parameters of the Ternary Orthorhombic Subcarbide Solid Solution .

(15-50-35), as presented in Figures 14 and 15, show thermal arrests at 1780°C and 1820°C respectively. These thermal arrests are most probably due to the stabilization of the high-temperature modification of the subcarbide phase, (i.e. hexagonal structure with a destruction of long-range order in the carbon sublattice) by V_2C . For several alloys at the same carbon concentration, i.e. 35 atomic %, but richer in vanadium content, no thermal arrest was observed by DTA-method under similar experimental conditions. Based on the DTA results, the appearance of the ternary high-temperature disordered phase (β') at 1780°C may be attributed to a formation from the monocarbide phase (γ) and the low-temperature hexagonal subcarbide phase (β) in a pseudobinary eutectoid reaction as follows:

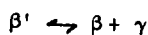


Figure 16 shows the reaction sequence starting from T_1 , (1780°C) at which β' is first formed to T_2 (slightly above 2440°C) where the two-phase field β - β' disappears in the binary niobium-carbon system. A second and equally possible reaction sequence, which is favored in the present work, will be described in a later section on the assembly of the ternary phase diagram.

2. Phase Equilibria in the Melting Range

The location of the eutectic trough, extending from the vanadium side at 15 atomic % C to the niobium side at 10.5 atomic % C, was established by metallographic examination of alloys having carbon concentrations between 13 and 20 atomic %. The photomicrographs of three alloys — V-Nb-C (75-5-20), V-Nb-C (70-15-15), and V-Nb-C (60-23-17) — near the metal-subcarbide eutectic trough are shown in Figures 17, 18, and 19. Figure 17 exhibits the primary subcarbide with metal precipitations within these grains and the metal-rich eutectic-like structure. Figure 18 shows an eutectic-type structure indicating the alloy V-Nb-C (60-23-17) is on the eutectic trough, and the third photomicrograph as presented in Figure 19 again depicts the primary subcarbide phase and the metal-rich eutectic-type structure. The fact that all three alloys exhibit eutectic-like structure indicates the three-phase boundaries must be extremely narrow, in agreement with the

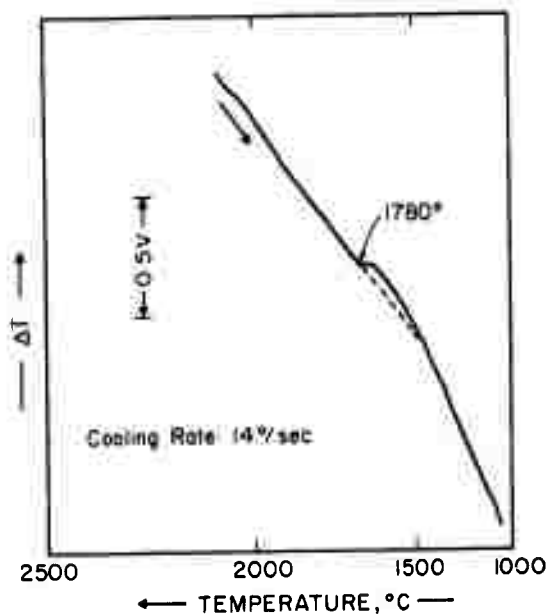


Figure 14. DTA-Thermogram of a V-Nb-C (25-40-35) Alloy

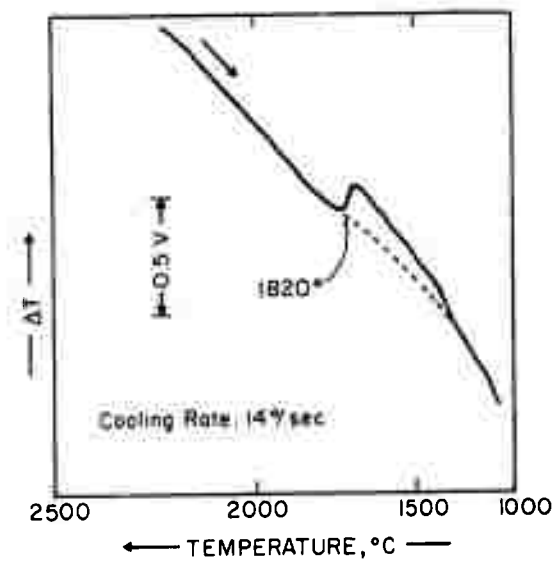


Figure 15. DTA-Thermogram of a V-Nb-C (15-50-35) Alloy

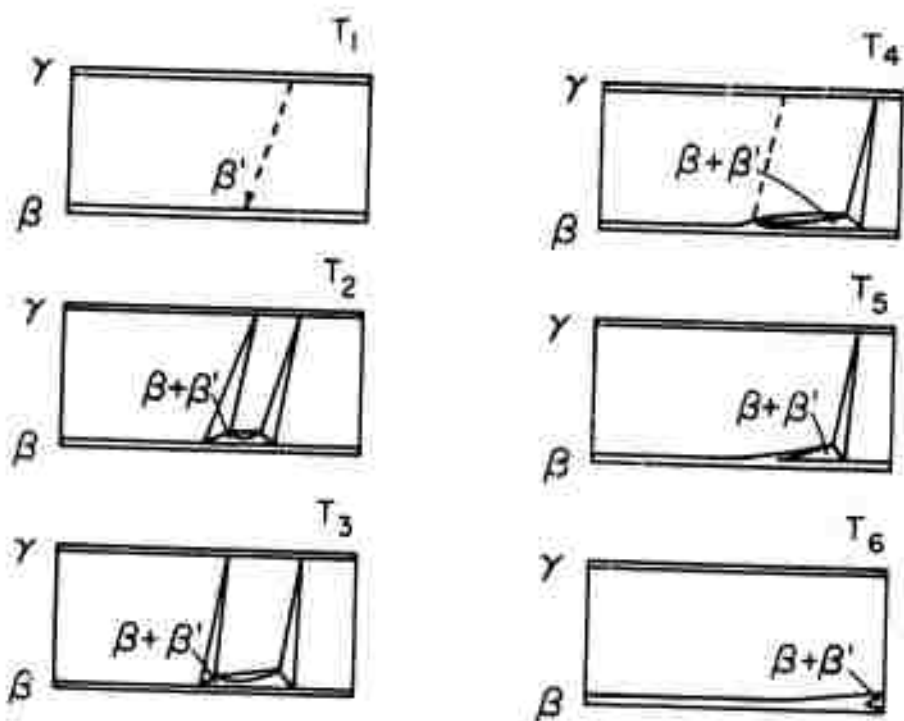


Figure 16. V-Nb-C: Schematic Illustration of the Optional Reaction Scheme for the Formation of the β' -(V,Nb)₂C Phase.



Figure 17. Photomicrograph of a V-Nb-C (70-5-20) Alloy Quenched from About 1670°C. X600

Primary Subcarbide Phase with Metal Precipitates within the Grains and Metal-Rich Eutectic Structure.

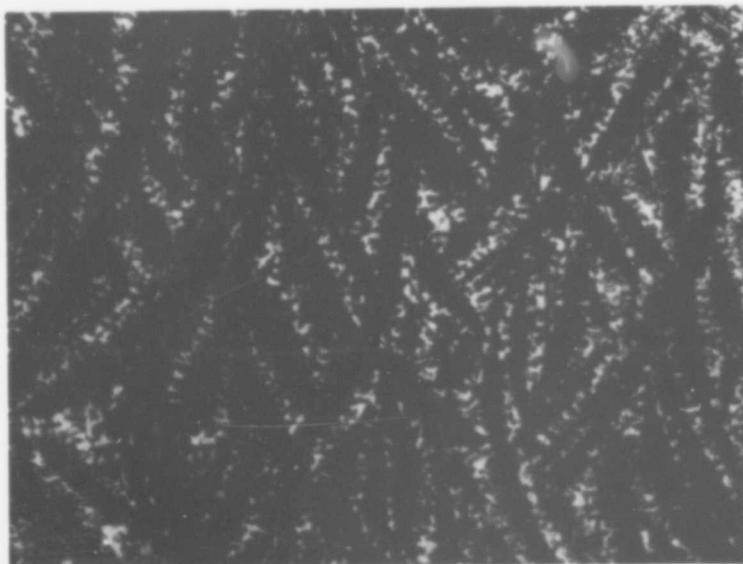


Figure 18. Photomicrograph of an Arc-Melted V-Nb-C (70-15-15) Alloy. X720

Metal-Rich Eutectic-Type Structure.

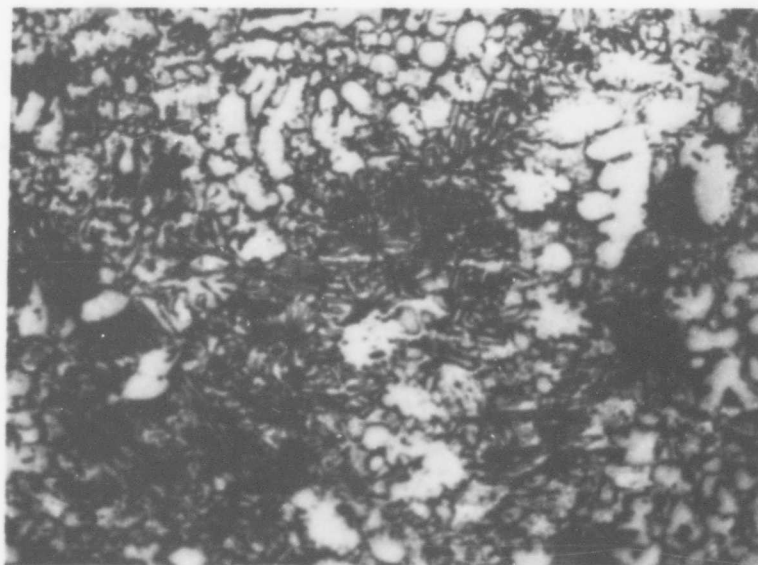


Figure 19. Photomicrograph of an Arc-Melted V-Nb-C (60-23-17) Alloy. X1000

Primary Subcarbide and Metal-Rich Eutectic-Type Structure.

sharp melting observed in the melting point determination as shown in Figure 20. With increased niobium-exchange, the melting became less sharp as shown in Figure 20, indicating the boundaries of the three-phase equilibria became wider. Eutectic like structures were not obtained for any of these alloys. Figures 21 and 22 show two photomicrographs of arc-melted niobium-richer alloys — V-Nb-C (50-35-15) and V-Nb-C (22-65-13) — exhibiting typical two-phase structures of metal and subcarbide.

The ternary subcarbide solid solution $(V, Nb)_2C$ melts peritectically in a similar manner as the pure V_2C and Nb_2C . The peritectic temperatures and carbon compositions of alloys determined in the present study are presented in Figure 23. The data for pure V_2C and Nb_2C according to Rudy, Windisch, and Brukl⁽¹⁾ are also included in this figure. Several of the alloys, as shown in Figure 23, had rather low incipient melting points, most probably due to the presence of unreacted monocarbide-metal mixture in the melting point samples. Three typical photomicrographs showing the

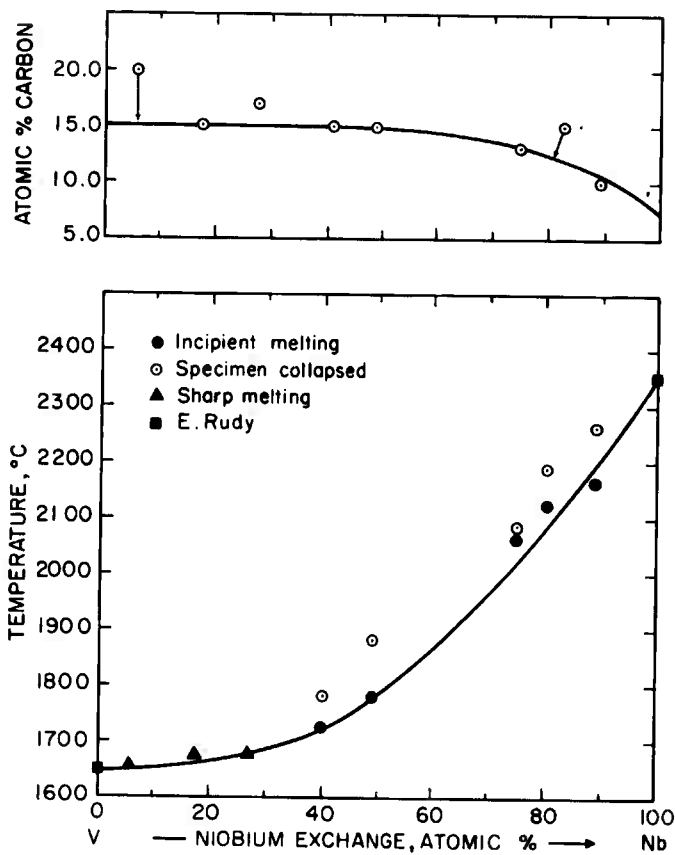


Figure 20. Compositions and Melting Temperatures of the Metal-Rich Eutectic Trough.



Figure 21. Photomicrograph of an Arc-Melted V-Nb-C (50-35-15) Alloy. X100
Two-Phase, Metal and Subcarbide.

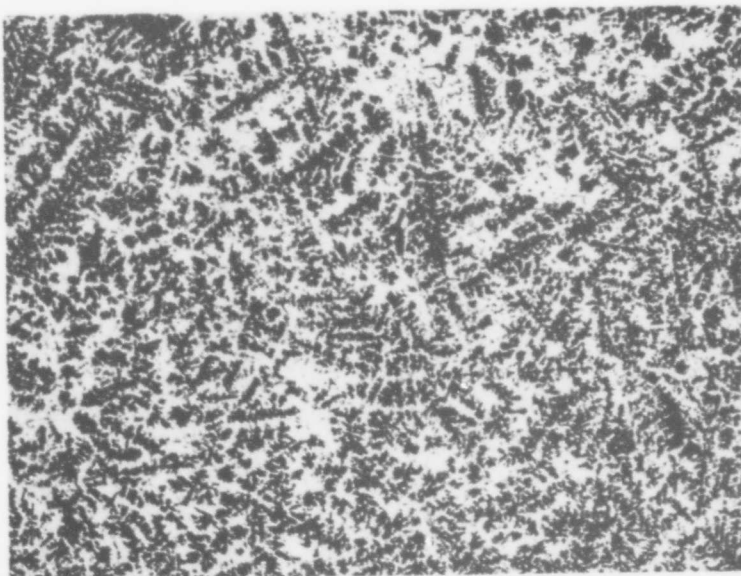


Figure 22. Photomicrograph of an Arc-Melted V-Nb-C (22-65-13) Alloy. X100
Two-Phase, Metal and Subcarbide.

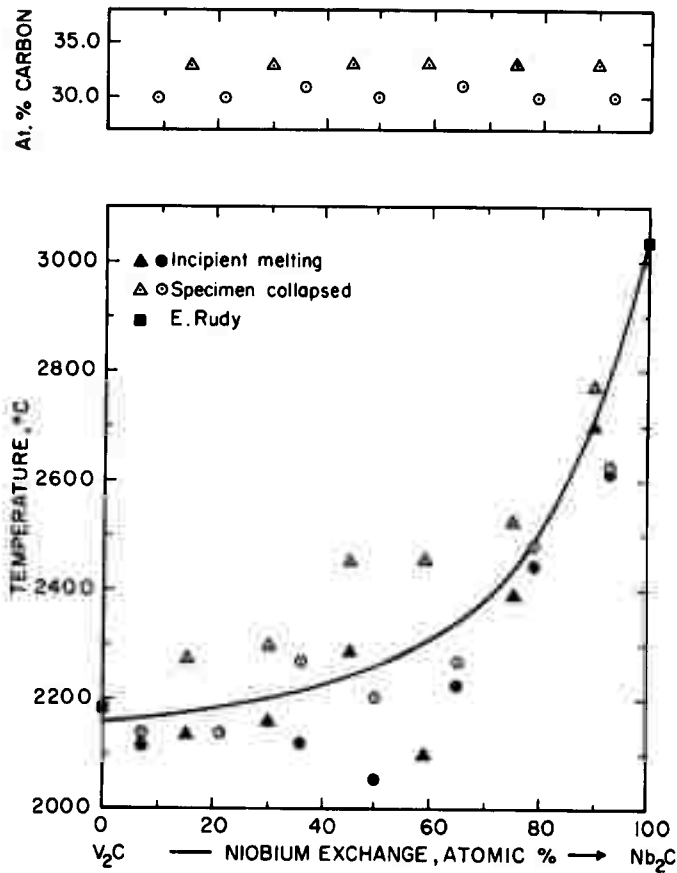


Figure 23. Compositions and Peritectic Temperatures of the Ternary Subcarbide Phase.

peritectic-type reactions are presented in Figures 24 through 26. Figure 24 shows the monocarbide grains being attacked by the metal solutions to form the subcarbide phase; while the two niobium-rich alloys as presented in Figures 25 and 26, also exhibit the precipitation of the subcarbide phases within the monocarbide grains.

The Pirani melting point data of the ternary monocarbide alloys are presented in Figure 27 as a function of niobium-exchange for different compositions of carbon. As shown in Figure 27, the solidus temperatures of the monocarbide solid solution increase smoothly from the vanadium-side to the niobium side. With the exception of alloys close to the two binary phases VC and NbC, melting of the ternary monocarbide phase was extremely heterogeneous as also presented in Figure 27,

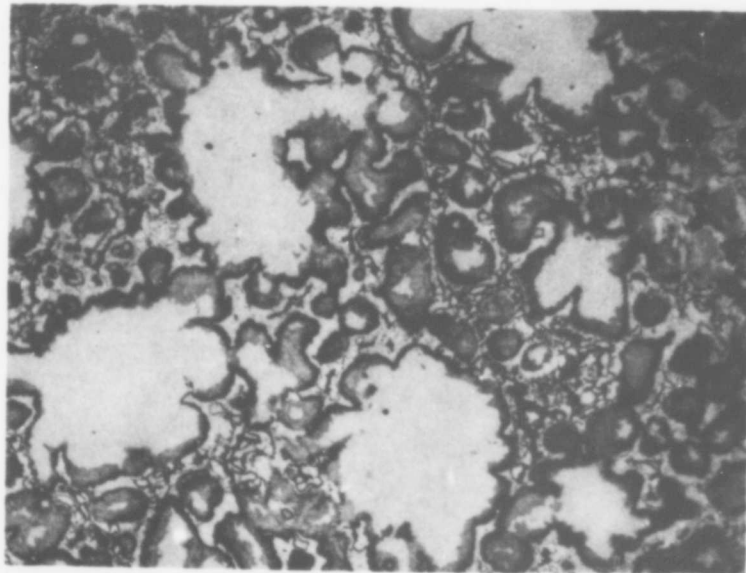


Figure 24. Photomicrograph of a V-Nb-C (37-30-33) Alloy Quenched from About 2500°C.

X250.

Monocarbide, Metal, and Subcarbide.



Figure 25. Photomicrograph of a V-Nb-C (15-55-30) Alloy
Quenched from About 2500°C.

X475

Monocarbide, Metal, and Subcarbide with Subcarbide
Precipitates within the Monocarbide Grains.

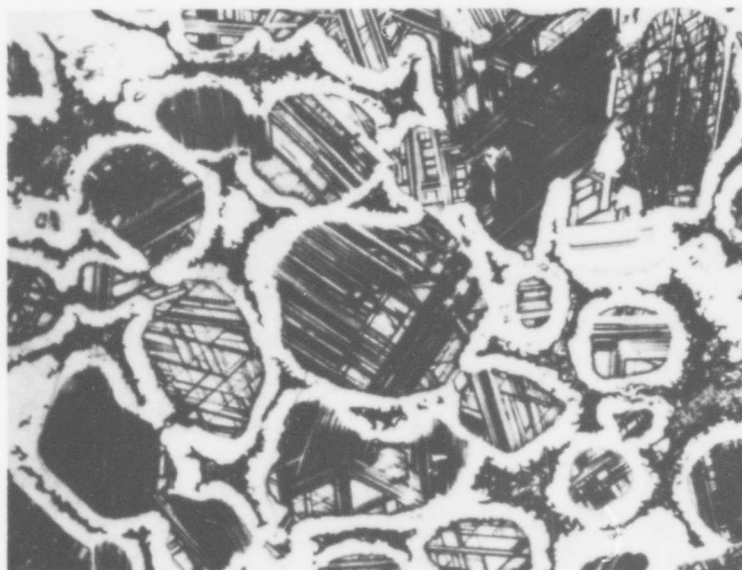


Figure 26. Photomicrograph of a V-Nb-C (7-60-33) Alloy
Quenched from about 2800°C.

X375

Monocarbide, Metal, and Subcarbide with Subcarbide Precipitates
within the Monocarbide Grains.

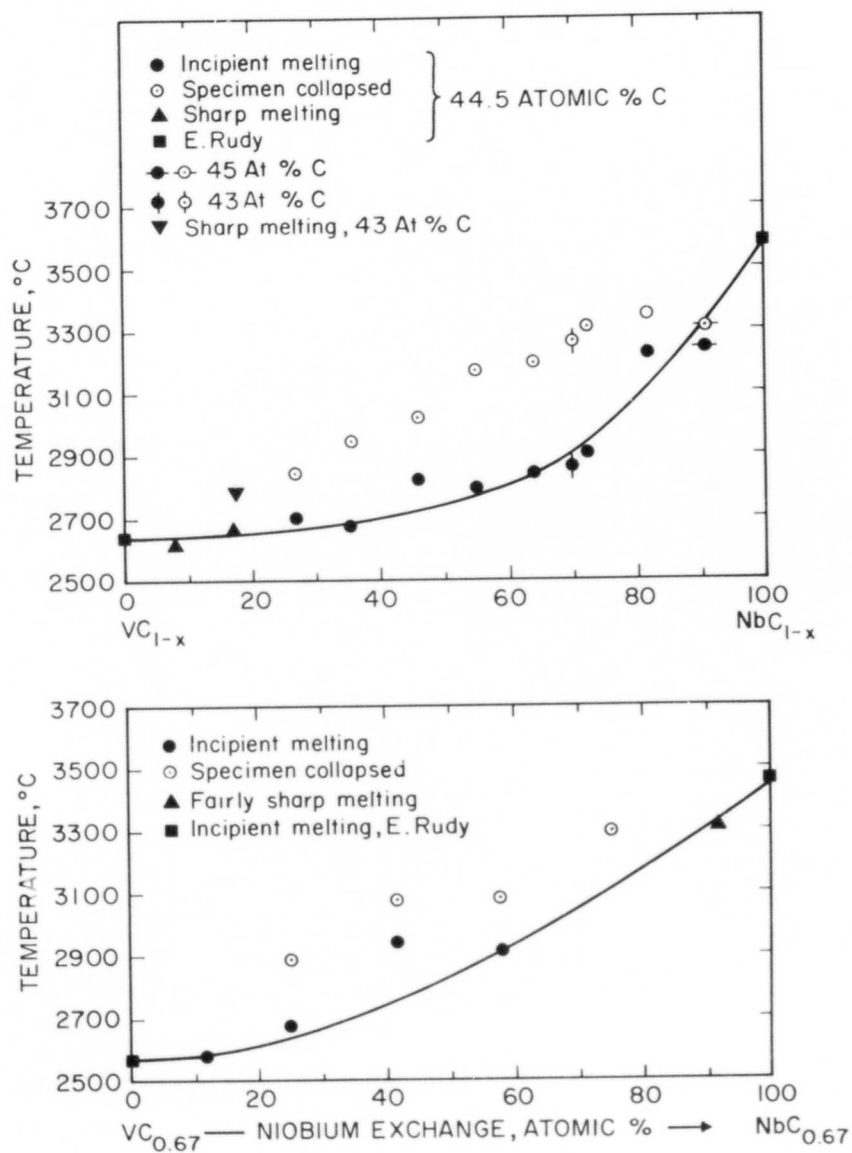


Figure 27. Pirani Melting Point Data of the Ternary Monocarbide Alloys.

indicating a wide separation of the solidus and liquidus surfaces. The top portion of Figure 23 shows, within the scatter of the data and the limited number of melting point determinations, that the maximum solidus temperatures of the monocarbide phase for carbon concentrations varying from 43 to 45 atomic % are essentially the same. Two typical photomicrographs of the monocarbide phase having compositions close to the two binary phases show single-phase alloys. These are presented in Figures 28 and 29.

The temperatures and compositions of the carbon-rich eutectic trough are presented in Figure 30. Starting from the vanadium-side, the temperatures increase gradually up to about 50 atomic % and then increase sharply toward the binary carbon-rich eutectic in the niobium-carbon binary. Figure 31 shows the photomicrograph of a V-Nb-C (46-4-54) alloy quenched from 2650°C exhibiting the primary crystallization of graphite. On the other hand, Figure 32, a photomicrograph of V-Nb-C (3-40-57) alloy quenched from 3200°C, shows the primary monocarbide phase and the graphite-monocarbide eutectic like structure.

3. Assembly of the Phase Diagram

The experimental evidence, as presented, is summarized in the ternary constitutional diagram vanadium-niobium-carbon (Figure 1) from 1400°C through the melting range of the monocarbide solid solutions. The equilibria below 1400°C are not included in this phase diagram, since the phase relationships at low-temperatures were not extensively investigated. To facilitate reading of the three-dimensional phase diagram, a series of isothermal sections were prepared and are shown in Figures 33 through 42. The reaction sequence for the initiation of the $\beta'-(V,Nb)_2C$ phase in the ternary at 1780°C and the termination of the same phase in the niobium-carbon binary, as favored in the present work, is presented in Figures 35 through 41. Finally, the liquidus projections which are consistent with the binary systems and the isothermal sections are presented in Figure 42.

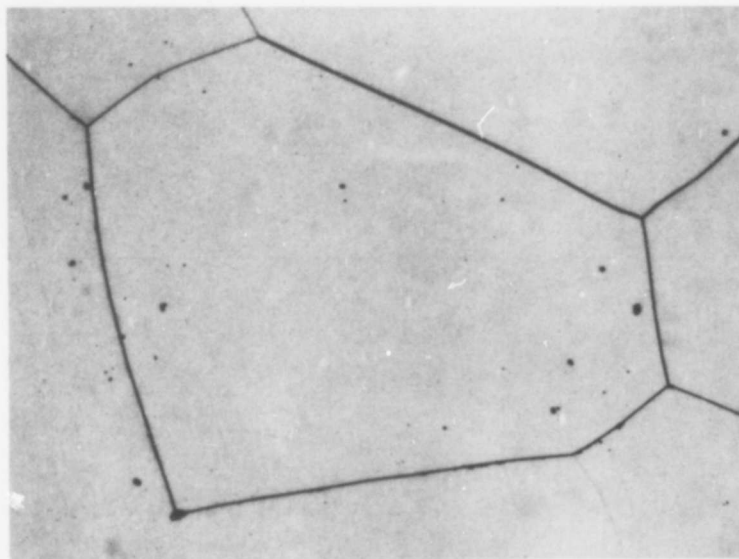


Figure 28. Photomicrograph of a V-Nb-C (5-55-40) Alloy
Quenched from about 2600°C.
Single-Phase Monocarbide .

X240

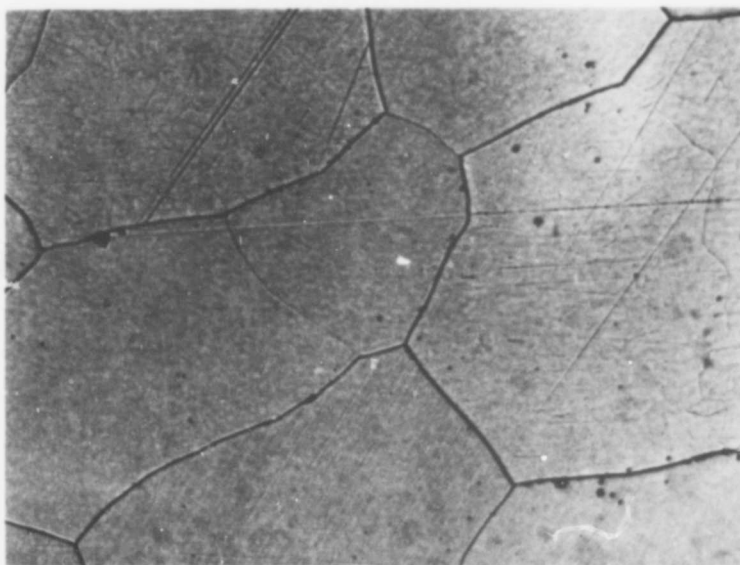


Figure 29. Photomicrograph of a V-Nb-C (5-50-45) Alloy
Quenched from about 3300°C.
Single-Phase Monocarbide.

X425

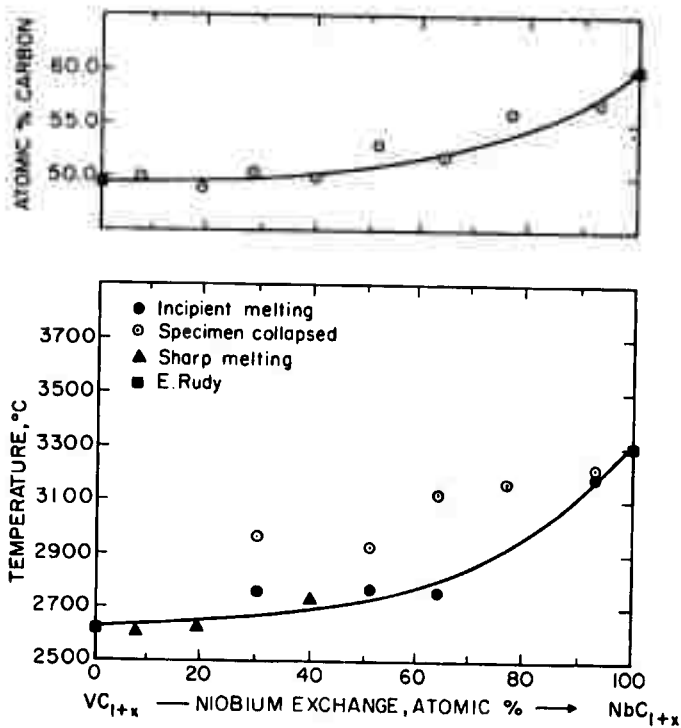


Figure 30. Compositions and Melting Temperatures of the Carbon-Rich Eutectic Trough.



Figure 31. Photomicrograph of a V-Nb-C (46-4-50) Alloy
Quenched from 2650°C.
Primary Graphite in a Monocarbide Matrix.

X400

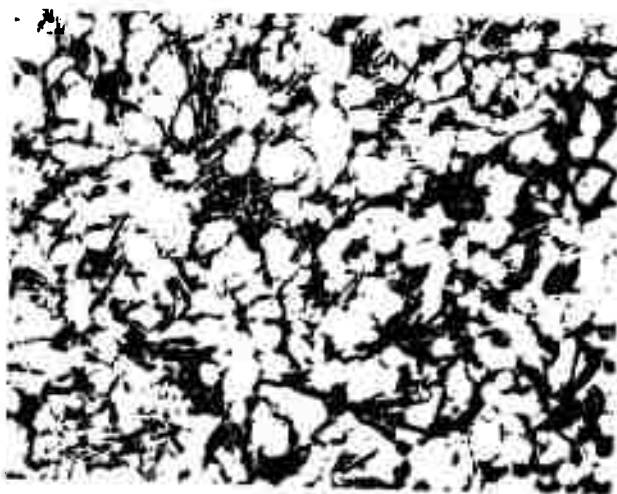


Figure 32. Photomicrograph of a V-Nb-C (3-40-57) Alloy
Quenched from 3200°C.

X135

Primary Monocarbide and Graphite-Monocarbide Eutectic.

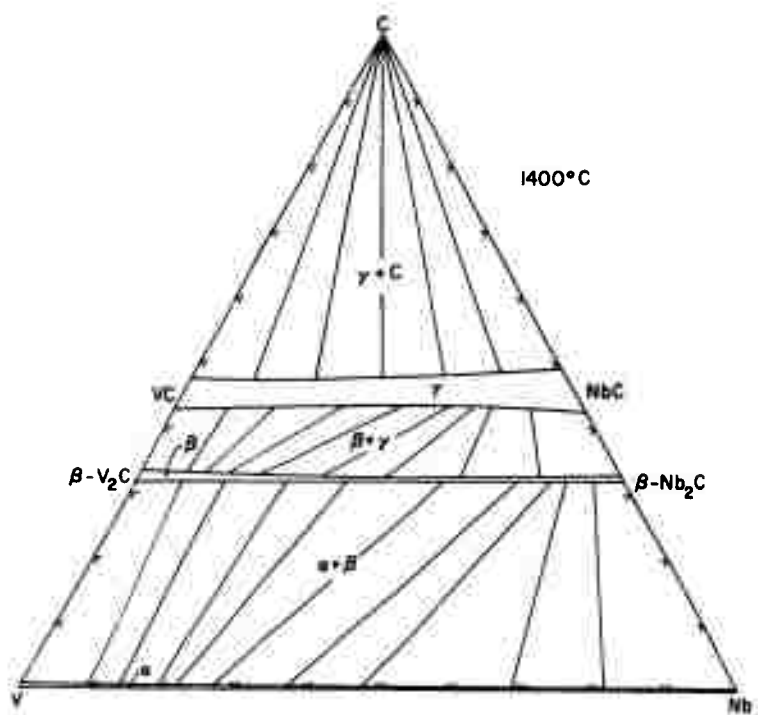


Figure 33. V-Nb-C. Isothermal Phase Equilibria at 1400°C.

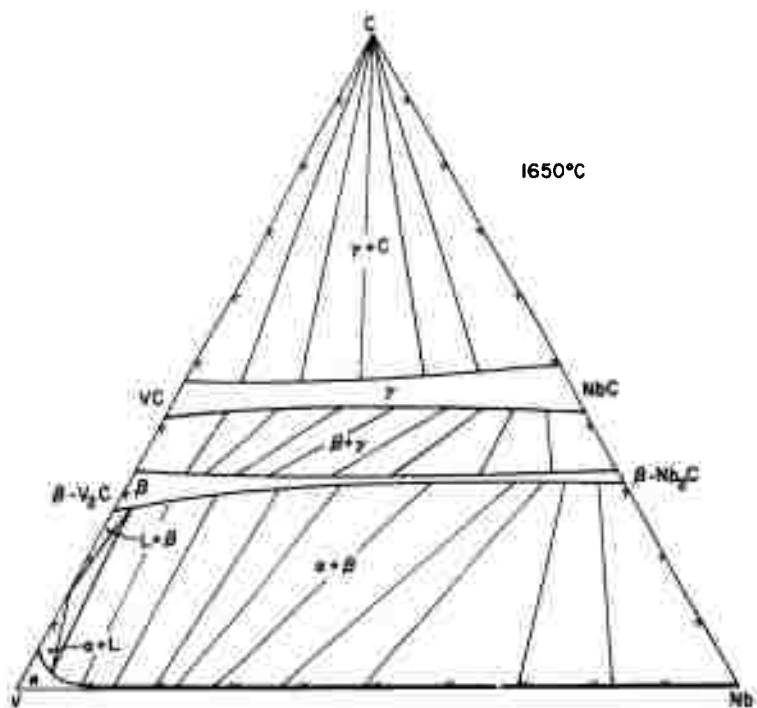


Figure 34. V-Nb-C. Isothermal Phase Equilibria at 1650°C.

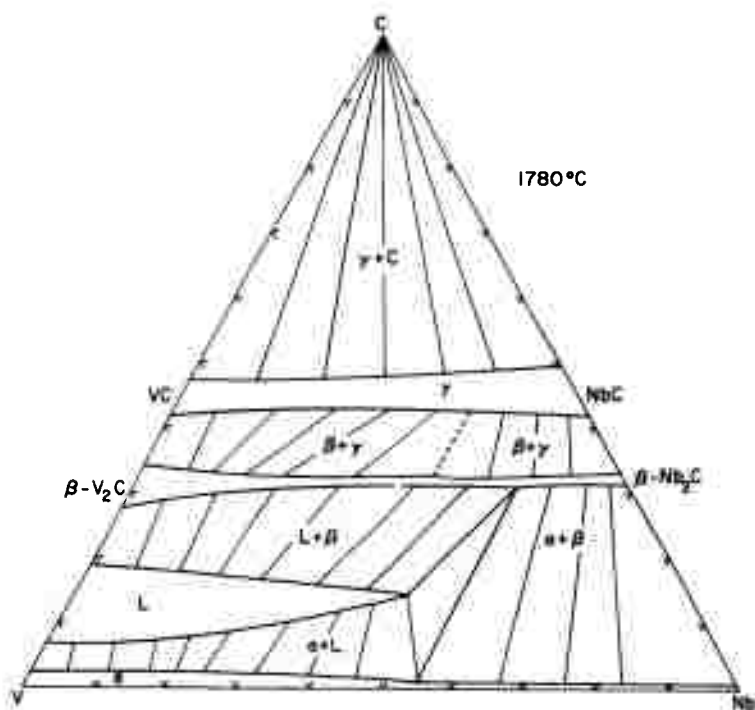


Figure 35. V-Nb-C. Isothermal Phase Equilibria at 1780°C.

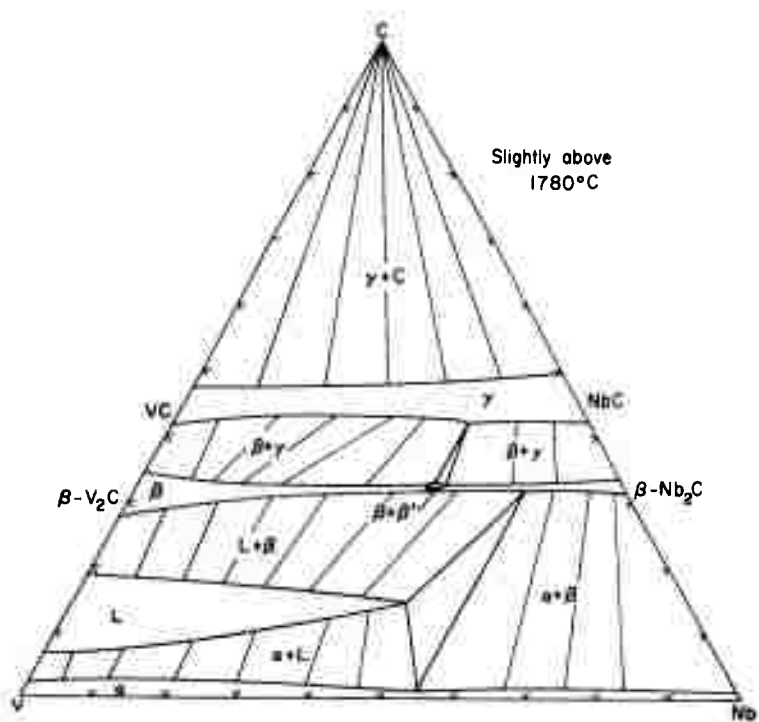


Figure 36. V-Nb-C. Isothermal Phase Equilibria at Slightly above 1780°C.

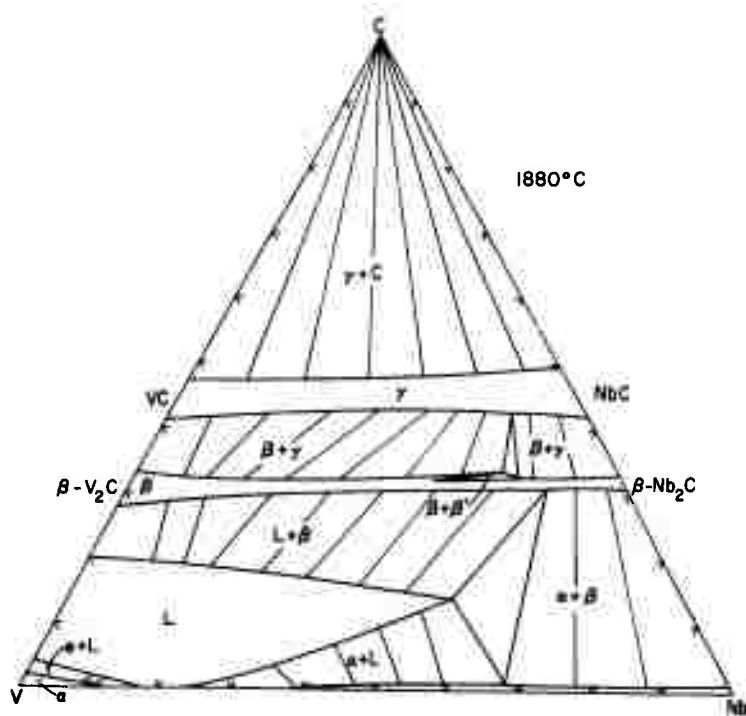


Figure 37. V-Nb-C. Isothermal Phase Equilibria at 1880°C.

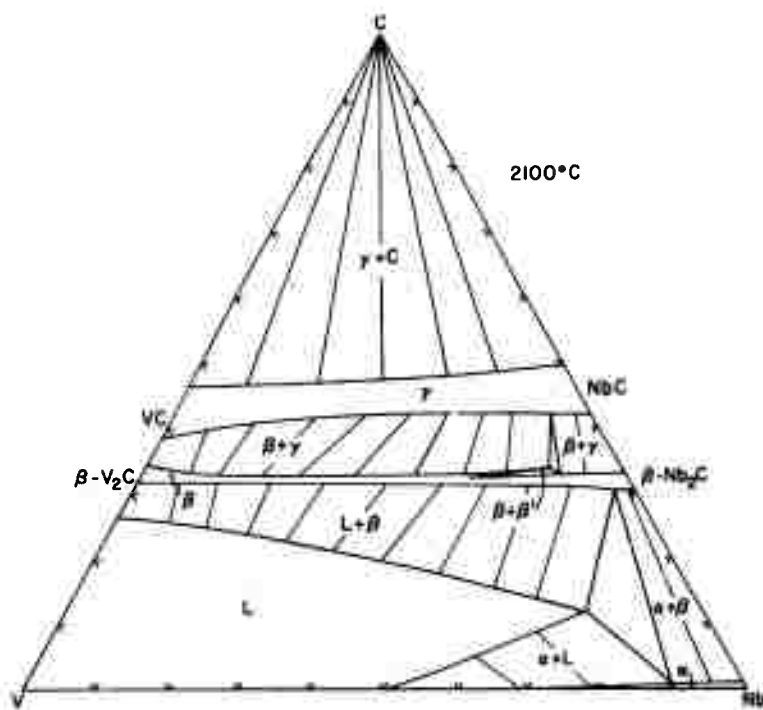


Figure 38. V-Nb-C. Isothermal Phase Equilibria at 2100°C.

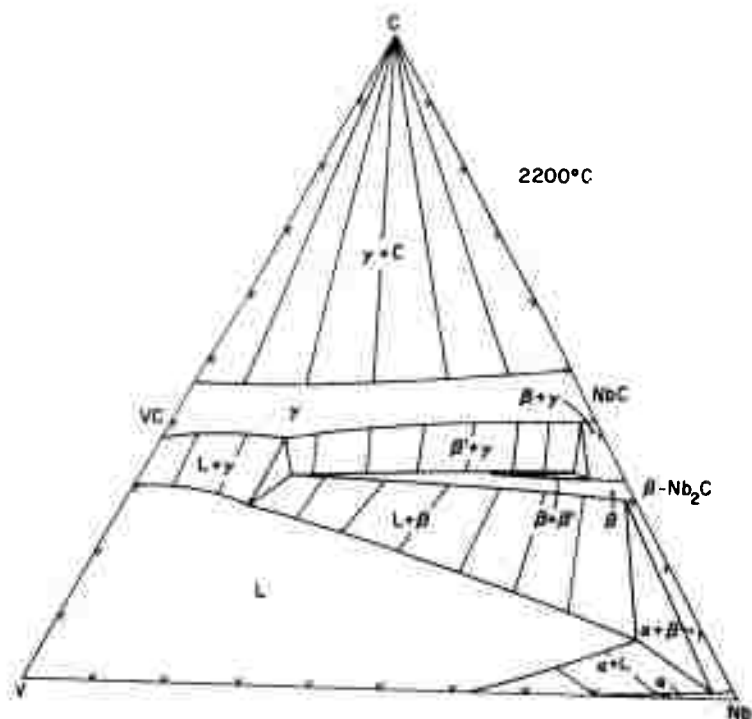


Figure 39. V-Nb-C. Isothermal Phase Equilibria at 2200°C.

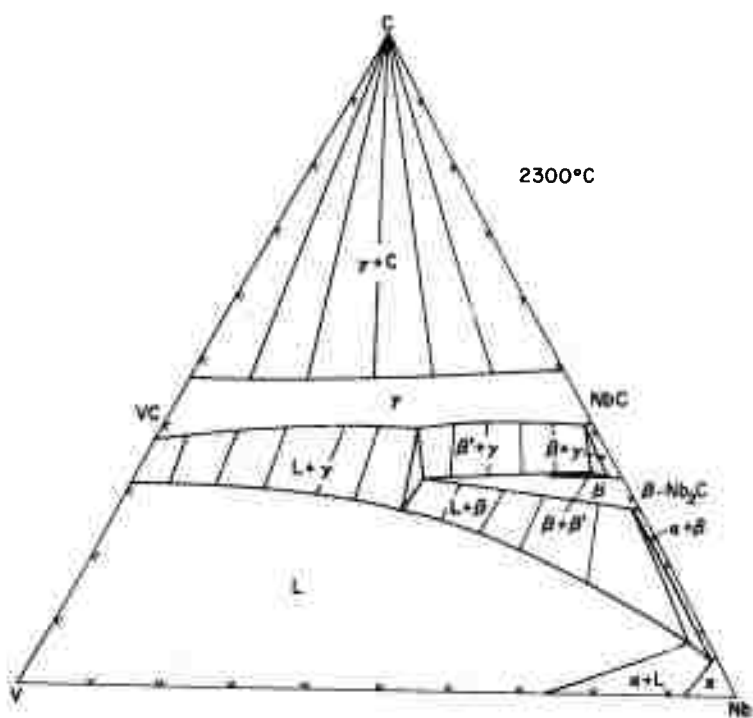


Figure 40. V-Nb-C. Isothermal Phase Equilibria at 2300°C.

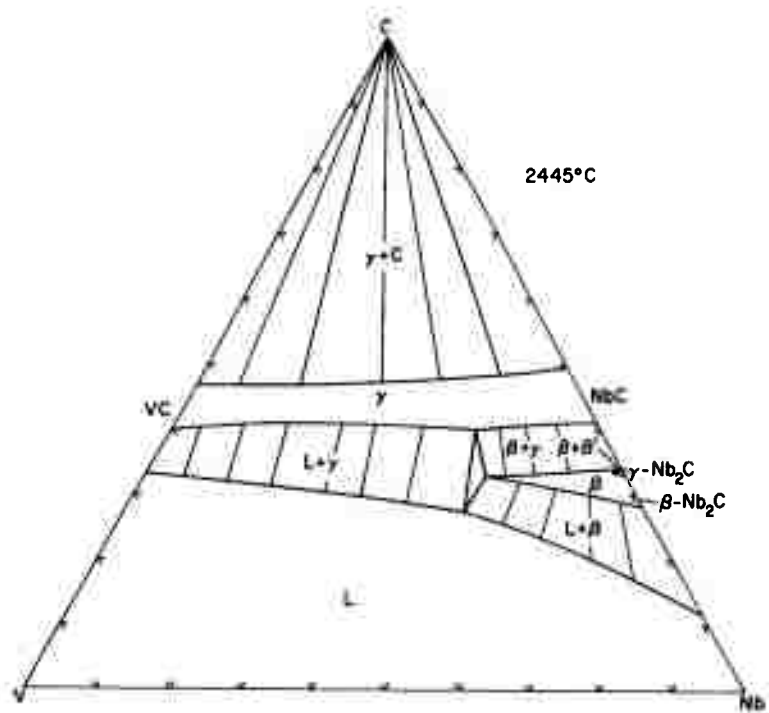


Figure 41. V-Nb-C. Isothermal Phase Equilibria at 2445°C.

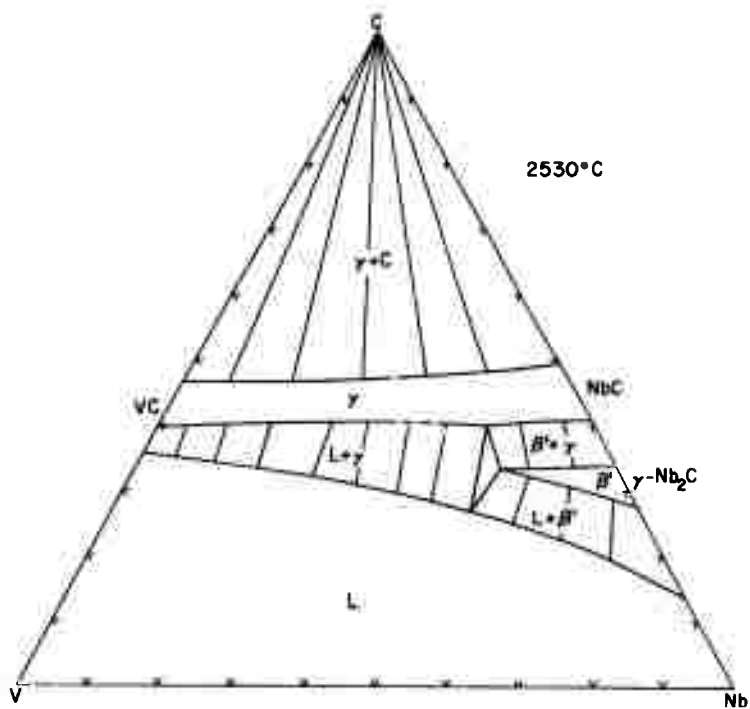


Figure 42. V-Nb-C. Isothermal Phase Equilibria at 2530°C.

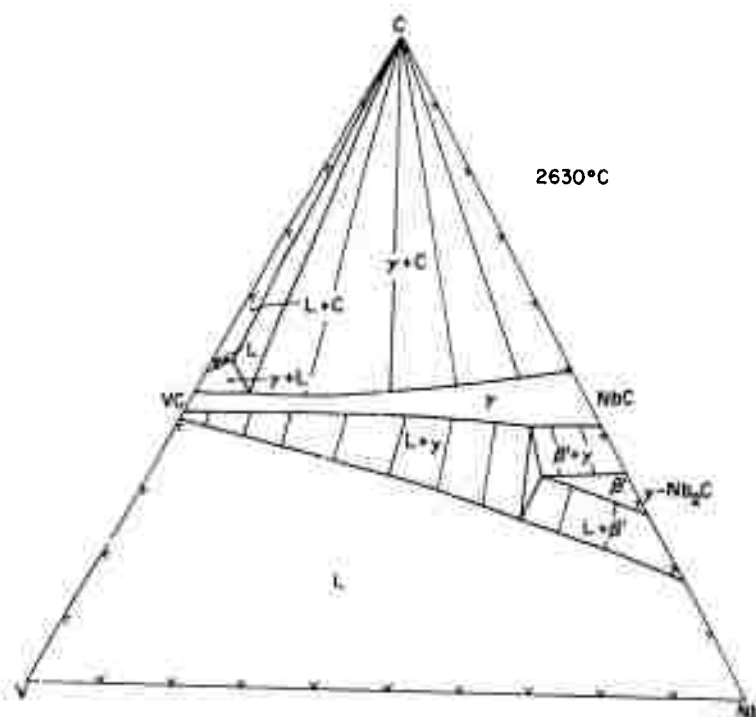


Figure 43. V-Nb-C. Isothermal Phase Equilibria at 2630°C.

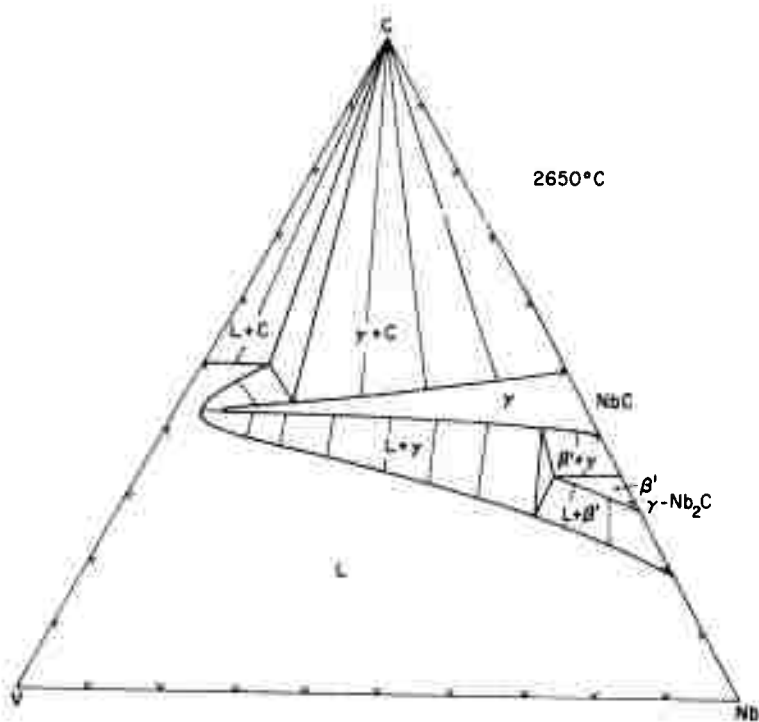


Figure 44. V-Nb-C. Isothermal Phase Equilibria at 2650°C.

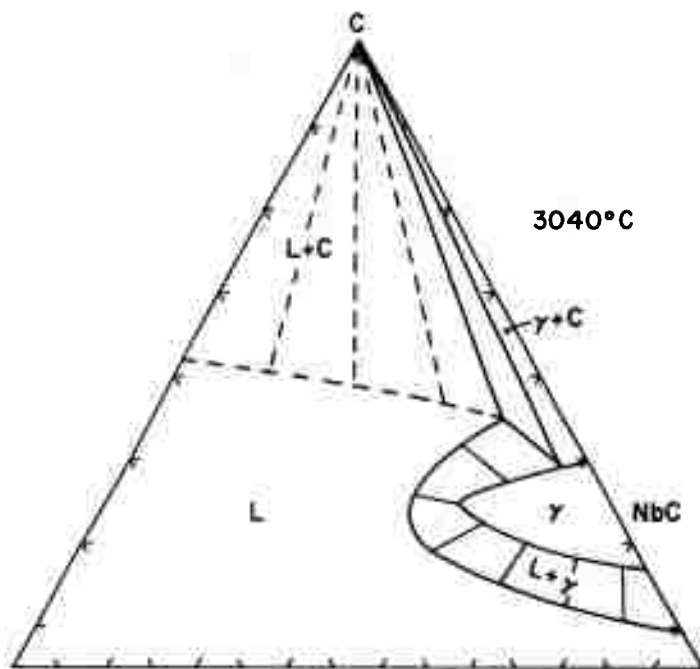


Figure 45. V-Nb-C. Isothermal Phase Equilibria at 3040°C.

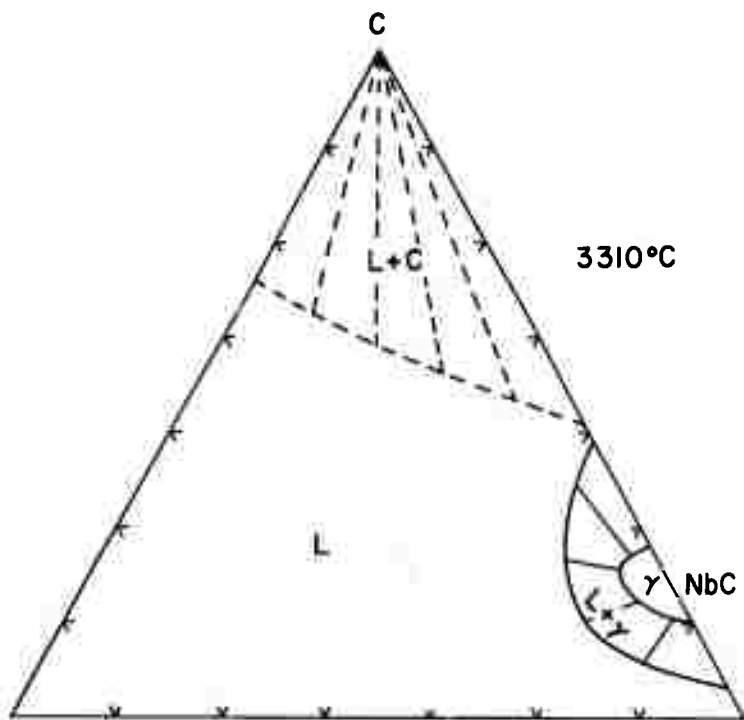
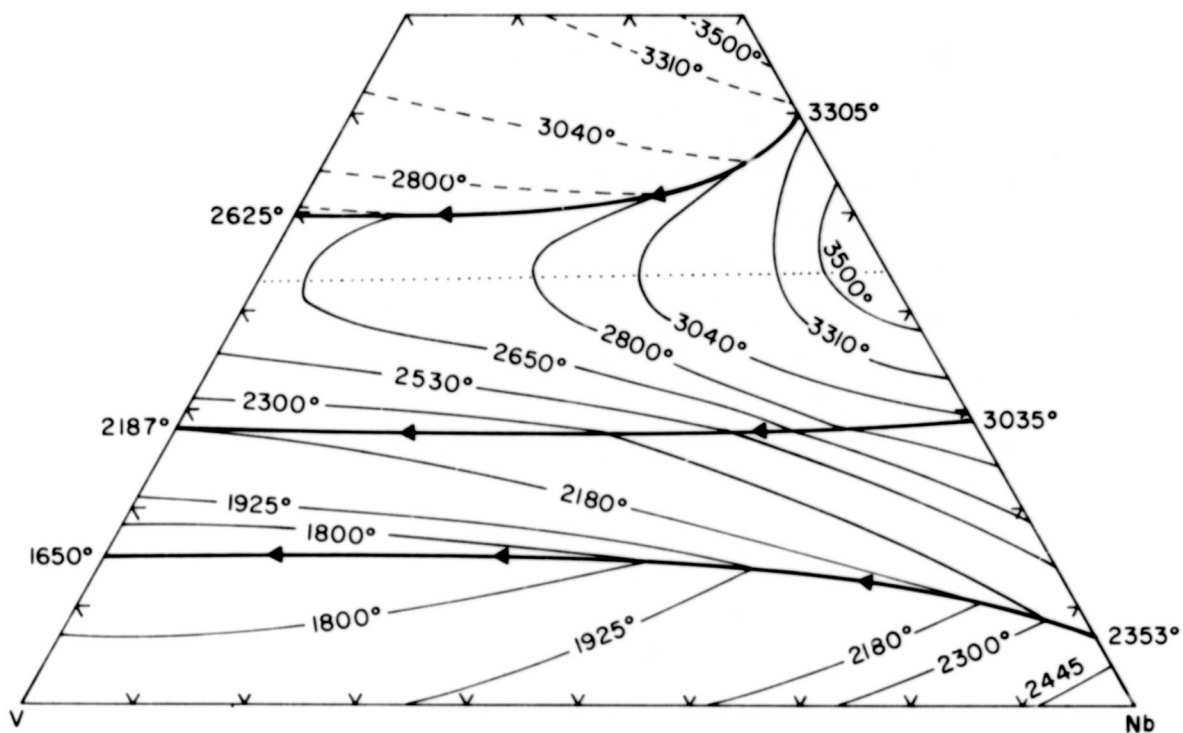


Figure 46. V-Nb-C. Isothermal Phase Equilibria at 3310°C.



..... Maximum Solidus Temperatures

Figure 47. V-Nb-C. Liquidus Projections.

IV. DISCUSSION

From the distributions of tie lines in the two-phase fields (V, Nb)-(V, Nb)₂C and (V, Nb)₂C-(V, Nb)C, one can derive the relative stabilities of V₂C versus Nb₂C and VC versus NbC, assuming the solution behaviors of the three series of solid solutions (V, Nb), (V, Nb)₂C and (V, Nb)C are known. The conditional equations governing the ternary phase equilibria have been extensively discussed by Rudy⁽¹³⁾. It was also shown that the ternary solid solution such as (V, Nb)C may be considered as a pseudo binary system consisting of VC and NbC. Moreover, regular solution model was found to be a good approximation for describing the solution behavior of these phases. The appropriate equation for two-phase equilibria between two series of solid solutions is

$$\frac{\delta \Delta G^a}{\delta x^a} = \frac{\delta \Delta G^b}{\delta x^b} \quad (1)$$

where ΔG^a is the Gibbs free energy of formation of the metal solid solution, (V, Nb), ΔG^b that of the subcarbide solid solution, x^a is the mole fraction of Nb in the metal phase, and x^b is that of Nb₂C in the subcarbide phase. Assuming the metal phase and the subcarbide phase behavior regularly, from equation (1) one obtains the Gibbs free energy difference between the two binary subcarbides VC and NbC as,

$$\Delta G_{f, NbC_{1/2}} - \Delta G_{f, VC_{1/2}} = RT \ln \frac{x^a}{1-x^a} \frac{1-x^b}{x^b} + \epsilon^a (1-2x^a) - \epsilon^b (1-2x^b)$$

where $\Delta G_{f, NbC_{1/2}}$ and $\Delta G_{f, VC_{1/2}}$ are respectively the Gibbs free energies of formation for^{1/2} the two binary^{1/2} subcarbide phases VC_{1/2} and NbC_{1/2} in cal/gatom metal, R is the universal gas constant, T is the absolute temperature, and ϵ^a and ϵ^b are respectively the interaction parameters for the metal and subcarbide solid solutions. From the shape of the solid-liquid phase boundaries in the metal binary, it is concluded that the metal solutions are

endothermic. Using the solubility parameters given by Brewer⁽¹⁴⁾, one obtains a value of about 100°K for the critical temperature of the metal binary solid solution. However, in view of the shape of the solid-liquid phase boundaries in the vanadium-niobium binary system, it is more likely that the critical temperature for a miscibility gap would be higher. Lattice parameters of alloys heat treated at 650°C for 113 hours by Wilhelm et al.⁽¹²⁾ showed that vanadium and niobium form a continuous series of solid solutions. Accordingly, a value of 800°K was taken as the critical temperature, which yielded a value of 3200 cal for the interaction parameter ϵ^a . Different values of ϵ^β varying from 4000 to 5600 cal/gatom metal were used to calculate the Gibbs free energy difference between $VC_{1/2}$ and $NbC_{1/2}$, but a value of 4800 cal/gatom metal fit the experimentally determined tie-line best. The value so obtained is $\Delta G_{f, NbC_{1/2}} - \Delta G_{f, VC_{1/2}} = -1900 \pm 550$ cal/gatom metal. The uncertainty includes only the scatter from the individual tie-line calculations. If one considers the uncertainties in the interaction parameters used, the uncertainty may be twice as large.

Based on this Gibbs free energy difference between $VC_{1/2}$ and $NbC_{1/2}$ and the tie-line distribution between $(V, Nb)C_{1/2}$ and $(V, Nb)C$ as determined at 1730°C and presented in Figure 9, one can obtain the relative stability between VC and NbC. From equation (1), one obtains the following relationship,

$$\begin{aligned} \Delta G_{f, NbC} - \Delta G_{f, VC} &= \Delta G_{f, NbC_{1/2}} - \Delta G_{f, VC_{1/2}} \\ &+ RT \ln \frac{x^\beta}{1-x^\beta} \frac{1-x^\gamma}{x^\gamma} + \epsilon^\beta (1-2x^\beta) - \epsilon^\gamma (1-2x^\gamma) \end{aligned} \quad (3)$$

In the above equation, $\Delta G_{f, NbC}$ and $\Delta G_{f, VC}$ are respectively the Gibbs free energies of formation for the NbC and VC phases, and x^γ is the mole fraction of NbC in the ternary $(V, Nb)C$ phase. Using the value of $\epsilon^\beta = 4800$ cal/gatom metal and assuming that the quantity, $\Delta G_{f, NbC_{1/2}} - \Delta G_{f, VC_{1/2}}$, is independent of temperature, i.e. $\Delta(\Delta S) = 0$, the free energy difference between NbC and VC may be evaluated using equation (3) and the tie-line distribution at 1730°C.

Varying values of ϵ^γ between 3200 and 4800 cal were used to evaluate equation (3), a value of $\epsilon^\gamma = 4400$ cal was found to fit the experimentally determined tie lines best. The value so obtained is $\Delta G_{f, \text{NbC}} - \Delta G_{f, \text{VC}} = -3000 \pm 600$ cal/gatom metal. Again the uncertainty of ± 600 cal is that due to the scatter of values obtained from individual tie lines only. However, when one considers all the other uncertainties involved, the overall uncertainty may be as much as ± 1500 cal/gatom metal.

From a recent compilation of the thermodynamic data of transition metal carbide as determined by conventional thermochemical means by Chang⁽¹⁵⁾, the Gibbs free energy difference between $\text{NbC}_{\sim 0.88}$ and $\text{VC}_{\sim 0.88}$ is -7000 ± 2000 cal/gatom metal. Even considering the large uncertainty associated with the value obtained in the present study and that with the literature value, the discrepancy is still rather large. The reason for this discrepancy is not clear and may be due to different value in the carbon to metal ratio. Since VC is susceptible to oxidation at ordinary temperature, the vanadium carbide used in the calorimetric determination might be contaminated with oxygen and thus would yield a value not sufficiently negative.

Based on the value of $\epsilon^\gamma = 4400$ cal/gatom metal, the monocarbide solid phase would form a miscibility gap at about 823°C. However, in view of the extremely slow kinetics for solution formation, no experiment was carried out to verify this temperature.

REFERENCES

1. E. Rudy, St. Windisch, and C.E. Brukl: U.S. Air Force Report AFML-TR-65-2, Part I, Vol. 12 (1967)
2. M. Hansen and K. Anderko: Constitution of Binary Alloys, 2nd Edition, McGraw-Hill, New York (1958).
3. E. Rudy: private communication (1967).
4. E. Rudy and C.E. Brukl: J.Am.Ceram.Soc. 50, No.5, 265 (1967).
5. R. Kieffer and F. Benesovsky: Hartstoffe, Wien, Springer (1963).
6. E.K. Storms & P.J. McNeal: J. Phys.Chem. 66, 1401 (1962).
7. E. Rudy and D.P. Harmon: U.S. Air Force Report, AFML-TR-65-2, Part I, Vol. V (Jan 1966).
8. See E.K. Storms: A Critical Review of Refractories, LA-2942 (1964).
9. E. Rudy: Z.Metallkd. 54, 213 (1963).
10. E. Rudy and G. Progulski: Planseeber Pulvermet., 15, No.1, p.13 (1967) and E. Rudy, St. Windisch, and Y.A. Chang: USAF Report AFML-TR-65-2, Part I, Vol.I (1965).
11. H.D. Heetderks, E. Rudy, and T.E. Eckert: Planseeber Pulvermet. 13 p.105 (1965), also USAF Report AFML-TR-65-2, Part IV, Vol. I (1965).
12. H.A. Wilhelm, O.N. Carlson, and J.M. Dickinson: J. Metals 6, 915, (1954).
13. E. Rudy: Z. Metallk. 54, 112 (1963).
14. L. Brewer: Prediction of High-Temperature Metallic Phase Diagram in High-Strength Materials, Edited by V. Zackay, John Wiley & Sons, New York (1965).
15. Y.A. Chang: USAF Report AFML-TR-65-2, Part IV, Vol. I (1965).

UNCLASSIFIED

Security Classification

DOCUMENT CONTROL DATA - R&D

(Security classification of title, body of abstract and indexing annotation must be entered when the overall report is classified)

1. ORIGINATING ACTIVITY (Corporate author) Aerojet-General Corporation Materials Research Laboratory Sacramento, California		2a. REPORT SECURITY CLASSIFICATION Unclassified	
		2b. GROUP N.A.	
3. REPORT TITLE Ternary Phase Equilibria in Transition Metal-Boron-Carbon-Silicon Systems Part II. Ternary Systems; Vol. XVI. V-Nb-C System			
4. DESCRIPTIVE NOTES (Type of report and inclusive dates)			
5. AUTHOR(S) (Last name, first name, initial) Chang, Y.A.			
6. REPORT DATE December 1967		7a. TOTAL NO. OF PAGES 54	7b. NO. OF REFS 15
8a. CONTRACT OR GRANT NO. AF 33(615)-1249		9a. ORIGINATOR'S REPORT NUMBER(S)	
a. PROJECT NO. 7350			
c. Task No. 735001		9b. OTHER REPORT NO(S) (Any other numbers that may be assigned this report) AFML-TR-65-2, Part II, Volume XVI	
10. AVAILABILITY/LIMITATION NOTICES Distribution of this document is unlimited. It may be released to the Clearinghouse, Department of Commerce, for sale to the General Public.			
11. SUPPLEMENTARY NOTES		12. SPONSORING MILITARY ACTIVITY AFML (MAMC) Wright-Patterson AFB, Ohio 45433	
13. ABSTRACT Phase equilibria in the ternary system vanadium-niobium-carbon from 800°C through the melting ranges of the cubic monocarbide solid solutions have been established on the basis of X-ray, melting point and metallographic studies. The phase equilibria above 1400°C are presented in a three-dimensional temperature-composition constitutional diagram, since the phase equilibria below 1400°C were not thoroughly investigated due to kinetic problems. Vanadium monocarbide and niobium monocarbide form a continuous series of solid solutions as do the low-temperature modification of the ordered hexagonal vanadium subcarbide and niobium subcarbide. However, the addition of vanadium subcarbide to niobium subcarbide stabilizes the high-temperature modification of the disordered hexagonal niobium subcarbide to about 1780°C in the ternary field.			

DD FORM 1 JAN 64 1473

UNCLASSIFIED

Security Classification

UNCLASSIFIED

Security Classification

14. KEY WORDS	LINK A		LINK B		LINK C	
	ROLE	WT	ROLE	WT	ROLE	WT
Ternary Metal-Metal-Carbon System High-Temperature Phase Equilibria						

INSTRUCTIONS

1. **ORIGINATING ACTIVITY:** Enter the name and address of the contractor, subcontractor, grantee, Department of Defense activity or other organization (*corporate author*) issuing the report.

2a. **REPORT SECURITY CLASSIFICATION:** Enter the overall security classification of the report. Indicate whether "Restricted Data" is included. Marking is to be in accordance with appropriate security regulations.

2b. **GROUP:** Automatic downgrading is specified in DoD Directive 5200.10 and Armed Forces Industrial Manual. Enter the group number. Also, when applicable, show that optional markings have been used for Group 3 and Group 4 as authorized.

3. **REPORT TITLE:** Enter the complete report title in all capital letters. Titles in all cases should be unclassified. If a meaningful title cannot be selected without classification, show title classification in all capitals in parentheses immediately following the title.

4. **DESCRIPTIVE NOTES:** If appropriate, enter the type of report, e.g., interim, progress, summary, annual, or final. Give the inclusive dates when a specific reporting period is covered.

5. **AUTHOR(S):** Enter the name(s) of author(s) as shown on or in the report. Enter last name, first name, middle initial. If military, show rank and branch of service. The name of the principal author is an absolute minimum requirement.

6. **REPORT DATE:** Enter the date of the report as day, month, year, or month, year. If more than one date appears on the report, use date of publication.

7a. **TOTAL NUMBER OF PAGES:** The total page count should follow normal pagination procedures, i.e., enter the number of pages containing information.

7b. **NUMBER OF REFERENCES:** Enter the total number of references cited in the report.

8a. **CONTRACT OR GRANT NUMBER:** If appropriate, enter the applicable number of the contract or grant under which the report was written.

8b, 8c, & 8d. **PROJECT NUMBER:** Enter the appropriate military department identification, such as project number, subproject number, system number, task number, etc.

9a. **ORIGINATOR'S REPORT NUMBER(S):** Enter the official report number by which the document will be identified and controlled by the originating activity. This number must be unique to this report.

9b. **OTHER REPORT NUMBER(S):** If the report has been assigned any other report numbers (*either by the originator or by the sponsor*), also enter this number(s).

10. **AVAILABILITY/LIMITATION NOTICES:** Enter any limitations on further dissemination of the report, other than those

imposed by security classification, using standard statements such as:

- (1) "Qualified requesters may obtain copies of this report from DDC."
- (2) "Foreign announcement and dissemination of this report by DDC is not authorized."
- (3) "U. S. Government agencies may obtain copies of this report directly from DDC. Other qualified DDC users shall request through _____."
- (4) "U. S. military agencies may obtain copies of this report directly from DDC. Other qualified users shall request through _____."
- (5) "All distribution of this report is controlled. Qualified DDC users shall request through _____."

If the report has been furnished to the Office of Technical Services, Department of Commerce, for sale to the public, indicate this fact and enter the price, if known.

11. **SUPPLEMENTARY NOTES:** Use for additional explanatory notes.

12. **SPONSORING MILITARY ACTIVITY:** Enter the name of the departmental project office or laboratory sponsoring (paying for) the research and development. Include address.

13. **ABSTRACT:** Enter an abstract giving a brief and factual summary of the document indicative of the report, even though it may also appear elsewhere in the body of the technical report. If additional space is required, a continuation sheet shall be attached.

It is highly desirable that the abstract of classified reports be unclassified. Each paragraph of the abstract shall end with an indication of the military security classification of the information in the paragraph, represented as (TS), (S), (C), or (U).

There is no limitation on the length of the abstract. However, the suggested length is from 150 to 225 words.

14. **KEY WORDS:** Key words are technically meaningful terms or short phrases that characterize a report and may be used as index entries for cataloging the report. Key words must be selected so that no security classification is required. Identifiers, such as equipment model designation, trade name, military project code name, geographic location, may be used as key words but will be followed by an indication of technical content. The assignment of links, rules, and weights is optional.

UNCLASSIFIED

Security Classification